# An Approach to Improve Breast Cancer Detection by Using Various Strain Estimation Methods and Image Segmentation on Breast Ultrasound (BUS) Images

By

**Md. Maksud Alam (142467)**

**Shafiq Imtiaz (142459)**

**Noor Kutub Al Hasan (142471)**

**Fahad Bin Sarwar (142449)**

A Thesis Submitted to the Academic Faculty in Partial Fulfillment of the Requirements for the Degree of

**BACHELOR OF SCIENCE IN ELECTRICAL AND ELECTRONIC ENGINEERING**


Department of Electrical and Electronic Engineering

**Islamic University of Technology (IUT)**

Gazipur, Bangladesh

November 2018

## Certificate of Approval

The thesis titled “An Approach to Improve Breast Cancer Detection by Using Various Strain Estimation Methods and Image Segmentation on Breast Ultrasound(BUS) Images” submitted by Md. Maksud Alam, Shafiq Imtiaz, Noor Kutub Al Hasan and Fahad Bin Sarwar bearing Student No. 142467, 142459, 142471, 142449 respectively of Academic Year 2017-2018 has been found as satisfactory and accepted as partial fulfillment of the requirement for the degree of Bachelor of Science in Electrical and Electronic Engineering on, 2018.

---------- (Supervisor)
Prof. Dr. Md. Ashraful Hoque

Head
Department of Electrical and
Electronic Engineering
Islamic University of Technology
Board Bazar, Gazipur-1704,
Bangladesh.

## Dedication

This thesis is dedicated to our beloved parents, teachers and all our well-wishers helping us to accomplish this work.

# Table of Contents

List of Figures ..... iv
List of Acronyms ..... v
Acknowledgment : ..... vi
Abstract: ..... vii
1 Introduction ..... 1
1.1 Breast Cancer Scenario: ..... 1
1.2 Breast Cancer detection procedure: ..... 2
1.2.1 Breast exam: ..... 2
1.2.2 Mammograms: ..... 2
1.2.2.1 Screening mammograms: ..... 2
1.2.2.2 Diagnostic mammograms: ..... 2
1.2.2.3 What do mammograms show? ..... 3
1.2.3 Removing a sample of breast cells for testing (biopsy) ..... 3
1.2.4 Magnetic resonance imaging (MRI) ..... 3
1.2.5 Ultrasound Imaging: ..... 6
1.2.6 Basic Principle of B Mode Ultrasound: ..... 7
1.2.7 Challenges in Ultrasound image interpretation: ..... 11
1.2.8 Ultrasound imaging in Breast cancer detection: ..... 11
1.3 Thesis Objectives ..... 13
1.4 Thesis Organization ..... 13
2 Background ..... 14
2.1 Related Work ..... 14
2.2 Overview of Proposed Method: ..... 16
3 Speckle and Noise Reduction using various filters ..... 17
3.1 Introduction: ..... 17
3.2 Application techniques: ..... 18
3.3 Filters used: ..... 18
3.3.1 MEDIAN FILTER: ..... 18
3.3.2 IDEAL FILTER: ..... 19
3.3.3 BUTTERWORTH FILTER: ..... 20
3.4 WAVELET FILTER: ..... 21
3.4.1 Wavelet properties: ..... 22

3.4.2 Working principle of wavelet filter: 22
3.4.3 Results: 23
3.5 HOMOMORPHIC WAVELET FILTERING: 25
3.5.1 Results: 26
4 Various Strain Estimation methods from Breast Ultrasound data 27
4.1 1D Shear elastography probe [31] 27
4.2 1D strain estimation (gradient) method: 29
4.3 1.5D strain estimator: 32
4.4 Short term correlation method: 36
4.5 Steps for Short term correlation algorithm: 40
4.6 Steps for Modified Short term correlation: 44
5 Adaptive stretching along with 2D strain estimation method 46
5.1 Adaptive Stretching 46
5.2 2D Strain estimation 47
5.3 METHOD OF APPLICATION: 48
5.4 Explanation of operation: 49
5.5 RESULTS: 51
6 Breast Lesion Segmentation 55
6.1 Ultrasound Image Segmentation: 55
6.2 Work Flowchart: 57
6.3 Gray level thresholding: 58
6.4 Automatic ROI generation 59
6.5 Edge Detection: 60
6.6 Results: 61
7 Conclusion and Future scope of research: 63
8 REFERENCES: 64

# List of Figures

Figure 1:1 A real MRI scanner ..... 4
Figure 1:2 Breast MRI ..... 5
Figure 1:3 Ultrasound image of a baby ..... 6
Figure 1:4 Formation of a 2D B-mode image. The image is built p line by line as the beam is stepped along the transducer array. ..... 8
Figure 1:5 Scan line arrangements for the most common B-mode formats ..... 9
Figure 1:6 Basic Pulse-Echo Ultrasound System (Image Courtesy: Dr. S. Kaisar Alam, Rutgers University, NJ, USA) ..... 10
Figure 1:7 B-mode image formation (Image Courtesy: Dr. S. Kaisar Alam, Rutgers University, NJ, USA) .. 10
Figure 3:1 Median filter on BUS: ( a ) Unfiltered image ( b ) Filtered image ..... 19
Figure 3:2 Ideal low pass filter on BUS: ( a ) Unfiltered image ( b ) Filtered image ..... 19
Figure 3:3 Butterworth filter on BUS: ( a ) Unfiltered image ( b ) Filtered image ..... 20
Figure 3:4 Wavelet filter on BUS, Case 1: ( a ) Unfiltered image ( b ) Filtered image ..... 23
Figure 3:5 Wavelet filter on BUS, Case 2: ( a ) Unfiltered image ( b ) Filtered image ..... 24
Figure 3:6 Wavelet filter on BUS, Case 3: ( a ) Unfiltered image ( b ) Filtered image ..... 24
Figure 3:7 Wavelet filter on BUS, Case 4: ( a ) Unfiltered image ( b ) Filtered image ..... 25
Figure 3:8 Homomorphic Wavelet filter on BUS : ( a ) Unfiltered image ( b ) Filtered image ..... 26
Figure 4:1 transient elastography probe ..... 27
Figure 4:2 Output from the probe ..... 28
Figure 4:3 Pre & Post Compressed window ..... 29
Figure 4:4 Overlapping Windows ..... 31
Figure 4:5 Output from Gradient method ..... 32
Figure 4:6 Lateral shifting windows ..... 34
Figure 4:7 axially shifted 1.5D window elements ..... 34
Figure 4:8 Output from 1.5D ..... 36
Figure 4:9 Short term correlation (without variable windows) ..... 37
Figure 4:10 Correlation matrix ..... 40
Figure 4:11 Displacement matrix ..... 41
Figure 4:12 Short term correlation with variable windows ..... 43
Figure 4:13 Mean results ..... 44
Figure 4:14 Median results ..... 45
Figure 5:1 Processed data at different applied: (a) at 1% strain (b) at 2% strain (c) at 4% strain ..... 52
Figure 5:2 Processed data at different post window size at 2% strain: (a) row size-8, column size-12 (b) row size-16, column size-24 (c) row size-32, column size-40 ..... 54
Figure 6:1 Case 1 ..... 61
Figure 6:2 Case 2 ..... 61
Figure 6:3 Case 3 ..... 61
Figure 6:4 Case 4 ..... 62
Figure 6:5 Case 5 ..... 62
Figure 6:6 Case 6 ..... 62

# List of Acronyms

| | |
|---|---|
| **B-mode** | Brightness-mode |
| **CAD** | Computer Aided Diagnosis |
| **FP** | False Positive |
| **FN** | False Negative |
| **MRI** | Magnetic Resonance Imaging |
| **ROI** | Region of Interest |
| **TP** | True Positive |
| **US** | Ultrasonography |
| **QUS** | Quantitative Ultrasound |

# Acknowledgment

First of all, we would like express our heartiest gratitude to the Almighty Allah for providing us the strength to complete this thesis work. After the Almighty, it is our great pleasure to express gratitude to the people who made this thesis possible.

Foremost, we would like to express our deepest gratitude to our supervisor, Prof. Dr. Md. Ashraful Hoque, Head, Dept. of EEE, IUT whose expertise, understanding and patience, added significantly to our graduate experience. This study could have never been done without our supervisors' motivation, guidance and inspiration.

We would also like to thank our mentor Dr. S. Kaisar Alam, Adjunct Professor, Rutgers University, NJ who sacrificed his valuable time for continuously guiding and motivating me for completing the thesis. He taught us how to work with the medical ultrasound imaging system and introduced me with the philosophical aspect of research which we will carry with us for the rest of my life.

We would like to acknowledge Dr. Juan Shan, Assistant Professor, Pace University, NY, USA, Prof. Dr. Dimitris Metaxas, Professor, Rutgers University, NJ, USA and Dr. Brian S. Garra. M.D., FDA, Silver Spring, MAD, USA for a number of stimulating discussions on the thesis. They enriched our understandings regarding the topic by sharing their valuable knowledge.

We would like to thank all the faculty members of EEE Dept., IUT for their continuous support and encouragement.

# Abstract

Breast cancer is the only cancer that is considered universal among women worldwide. Breast cancer is the most common cancer in American women, except for skin cancers. Currently, the average risk of a woman in the United States developing breast cancer sometime in her life is about 12%.

Breast cancer is sometimes found after symptoms appear, but many women with breast cancer have no symptoms. This is why regular breast cancer screening is so important. There is no sure way to prevent breast cancer.

Thus, early detection and treatment are crucial in minimizing breast cancer related deaths. Due to the inherent nature of ultrasound imaging such as uneven speckle patterns, no fixed threshold values, anisotropy and signal drop-out bio medical image processing is a challenging task. Automatic segmentation of BUS is very difficult due to uneven shape and imprecise boundary of breast lesions.

In order to improve the problem prevalent in the existing methods, a complete qualitative analysis of Breast ultrasound (BUS) images for tumor detection is proposed in this thesis. The method involves four steps – (a) Speckle reduction using different filters, (b) Strain estimation by various methods, (c) 2D search for displacement and then application of 1.5D adaptive stretching and (d) Image segmentation for lesion detection.

# 1 Introduction

## 1.1 Breast Cancer Scenario:

Breast cancer is the most commonly occurring cancer in women and the second most common cancer overall [1]. There were over 2 million new cases in 2018 [1]. Incidence rates vary greatly worldwide from 19.3 per 100,000 women in Eastern Africa to 89.7 per 100,000 women in Western Europe [2]. Belgium had the highest rate of breast cancer in women, followed by Luxembourg [1]. While most cases of breast cancer occur in women it does occur in men too, although this is rare (about 1% of cases) [3]. Breast cancer survival rates vary greatly worldwide, ranging from 80% or over in North America, Sweden and Japan to around 60% in middle-income countries and below 40% in low-income countries [4]. Breast cancer survival varies by stage at diagnosis. The overall 5-year relative survival rate is 99% for localized disease, 85% for regional disease, and 27% for distant-stage disease [5] Survival within each stage varies by tumor size. For example, among women with regional disease, the 5-year relative survival is 95% for tumors less than or equal to 2.0 cm, 85% for tumors 2.1-5.0 cm, and 72% for tumors greater than 5.0 cm [6]. Cause of breast cancer is still unknown to us. That's why early detection is very important for fruitful treatment.

## 1.2 Breast Cancer detection procedure:

Tests and procedures used to diagnose breast cancer include:

### 1.2.1 Breast exam:

The doctor will check both of the breasts and lymph nodes in the patient's armpit, feeling for any lumps or other abnormalities.

### 1.2.2 Mammograms:

Mammograms are low-dose x-rays that can help find breast cancer. A mammogram can often find or detect breast cancer early, when it's small and even before a lump can be felt. This is when it's easiest to treat. Types of Mammograms are given below.

#### 1.2.2.1 Screening mammograms:

A screening mammogram is used to look for signs of breast cancer in women who don't have any breast symptoms or problems. X-ray pictures of each breast are taken from 2 different angles.

#### 1.2.2.2 Diagnostic mammograms:

Mammograms can also be used to look at a woman's breast if she has breast symptoms or if a change is seen on a screening mammogram. When used in this way, they are called diagnostic mammograms. They may include extra views (images) of the breast that aren't part of screening mammograms. Sometimes diagnostic mammograms are used to screen women who were treated for breast cancer in the past.

#### 1.2.2.3 What do mammograms show?

Mammograms can often show abnormal areas in the breast. They can't prove that an abnormal area is cancer, but they can help health care providers decide whether more testing is needed. The 2 main types of breast changes found with a mammogram are calcifications and masses.

### 1.2.3 Removing a sample of breast cells for testing (biopsy)

A biopsy is the only definitive way to make a diagnosis of breast cancer [8]. During a biopsy, doctor uses a specialized needle device guided by X-ray or another imaging test to extract a core of tissue from the suspicious area. Often, a small metal marker is left at the site within patient's breast so the area can be easily identified on future imaging tests.

Biopsy samples are sent to a laboratory for analysis where experts determine whether the cells are cancerous. A biopsy sample is also analyzed to determine the type of cells involved in the breast cancer, the aggressiveness (grade) of the cancer, and whether the cancer cells have hormone receptors or other receptors that may influence your treatment options.

### 1.2.4 Magnetic resonance imaging (MRI)

MRI, or magnetic resonance imaging, is a technology that uses magnets and radio waves to produce detailed cross-sectional images of the inside of the body. MRI does not use X-rays, so it does not involve any radiation exposure. Breast MRI has a number of different uses for breast cancer, including:

- Screening high-risk women (women known to be at higher than average risk for breast cancer, either because of a strong family history or a gene abnormality)
- Gathering more information about an area of suspicion found on a mammogram or ultrasound
- Monitoring for recurrence after treatment

*Figure 1:1 A real MRI scanner*

Unlike a mammogram, which uses X-rays to create images of the breast, breast MRI uses magnets and radio waves to produce detailed 3-dimensional images of the breast tissue [9]. Before the test, patient may need to have a contrast solution (dye) injected into his arm through an intravenous line. Because the dye can affect the kidneys, doctor may perform kidney function tests before giving patient the contrast solution. The solution will help any potentially cancerous breast tissue show up more clearly. Some people experience temporary discomfort during the infusion of the contrast solution.

Cancers need to increase their blood supply in order to grow. On a breast MRI, the contrast tends to become more concentrated in areas of cancer growth, showing up as white areas on an otherwise dark background [9]. This helps the radiologist determine which areas could possibly be cancerous. More tests may be needed after breast MRI to confirm whether or not any suspicious areas are actually cancer.

MRI screening is not recommended for women whose lifetime risk of breast cancer is less than 15%. Studies indicates that although MRI is underutilized among high-risk women, it is often used in women who are not at high risk for breast cancer [10].

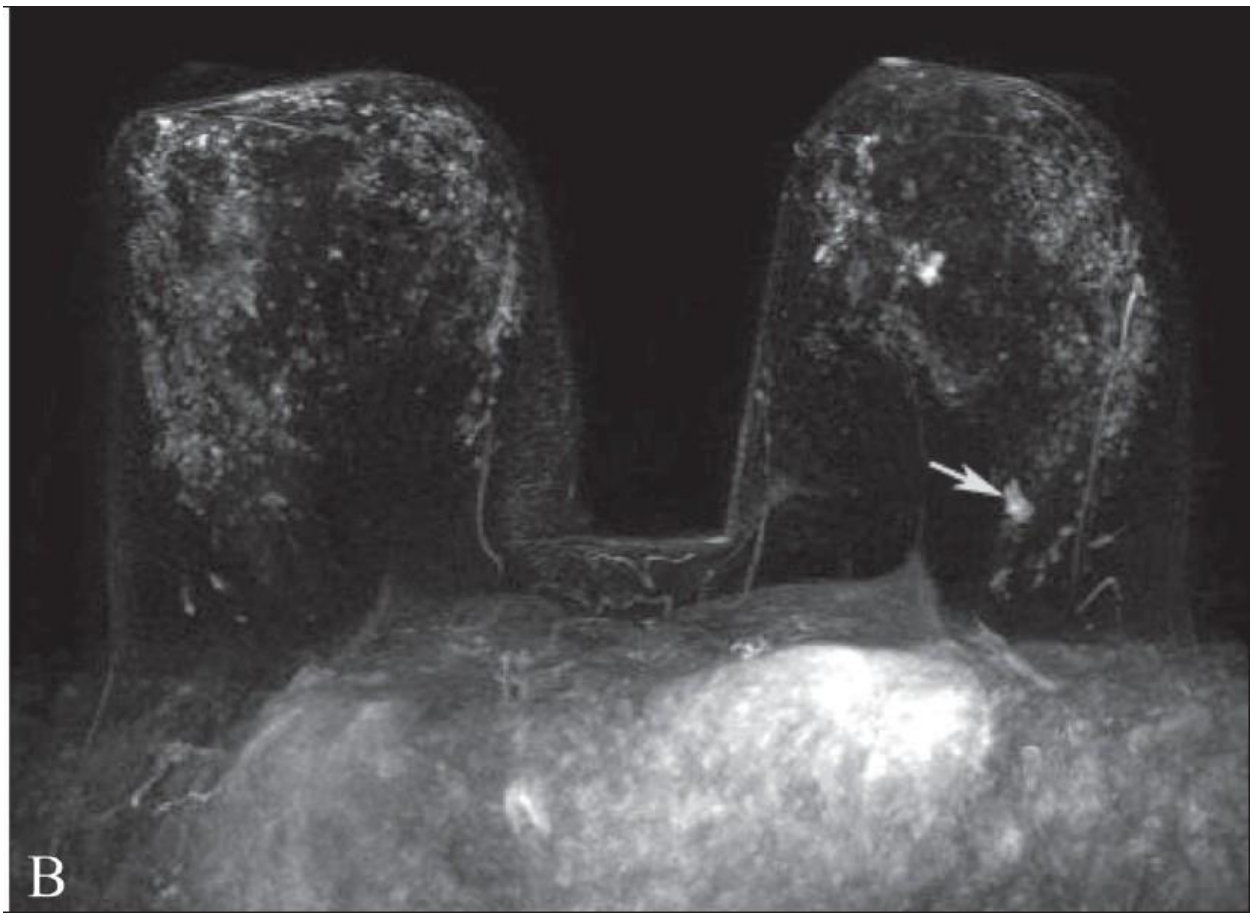


*Figure 1:2 Breast MRI*

### 1.2.5 Ultrasound Imaging:

Ultrasound imaging (sonography) is a diagnostic medical procedure that uses high-frequency sound waves to produce dynamic visual images of organs, tissues or blood flow inside the body. The sound waves are transmitted to the area to be examined and the returning echoes are captured to provide the physician with a 'live' image of the area. Ultrasound does not require the use of ionizing radiation, nor the injection of nephrotoxic contrast agents.

Ultrasound has several advantages which make it ideal in numerous situations, in particular, studies of the function of moving structures in real-time. It can be used to examine many parts of the body, such as the abdomen, heart and blood vessels, breasts, muscles, carotid arteries, and female reproductive system including pregnancy and prenatal diagnostics. Because of its non-ionizing nature, it is a good choice for imaging when radiation-sensitivity is a concern, such as in pediatrics or in women of child-bearing age.


*Figure 1:3 Ultrasound image of a baby*

### 1.2.6 Basic Principle of B Mode Ultrasound:

A B-mode image is a cross-sectional image representing tissues and organ boundaries within the body. It is constructed from echoes, which are generated by reflection of ultrasound waves at tissue boundaries, and scattering from small irregularities within tissues. Each echo is displayed at a point in the image, which corresponds to the relative position of its origin within the body cross section, resulting in a scaled map of echo-producing features. The brightness of the image at each point is related to the strength or amplitude of the echo, giving rise to the term B-mode (brightness mode). Usually, the B-mode image bears a close resemblance to the anatomy, which might be seen by eye, if the body could be cut through in the same plane. Abnormal anatomical boundaries and alterations in the scattering behavior of tissues can be used to indicate pathology.

To form a B-mode image, a source of ultrasound, the transducer, is placed in contact with the skin and short bursts or pulses of ultrasound are sent into the patient. These are directed along narrow beam-shaped paths. As the pulses travel into the tissues of the body, they are reflected and scattered, generating echoes, some of which travel back to the transducer, where they are detected. These echoes are used to form the image.

To display each echo in a position corresponding to that of the interface or feature (known as a target) that caused it, the B-mode system needs two pieces of information. These are

- The range (distance) of the target from the transducer and

- The direction of the target from the active part of the transducer, i.e. the position and orientation of the ultrasound beam.

The 2D B-mode image is formed from a large number of B-mode lines, where each line in the image is produced by a pulse–echo sequence. In early B-mode systems, the brightness display of these echoes was generated as follows.

As the transducer transmits the pulse, a display spot begins to travel down the screen from a point corresponding to the position of the transducer, in a direction corresponding to the path of the pulse (the ultrasound beam). Echoes from targets near the transducer return first and increase the brightness of the spot. Further echoes, from increasing depths, return at increasing times after transmission as the spot travels down the screen. Hence, the distance down the display at which each echo is displayed is related to its depth below the transducer. The rate at which the display spot travels down the screen determines the scale of the image. A rapidly moving spot produces a magnified image.

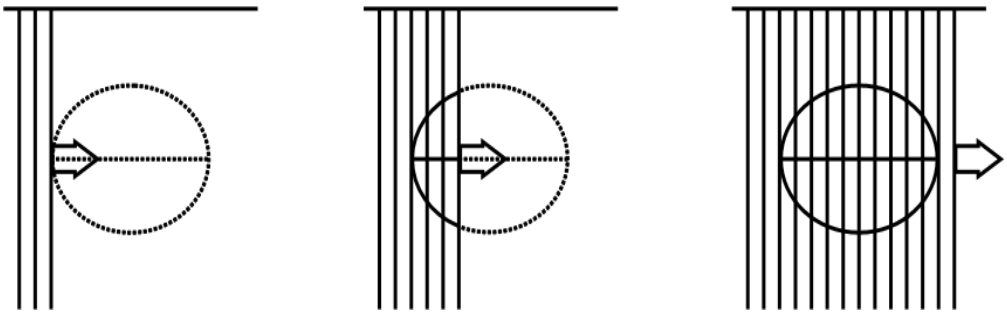

*Figure 1:4 Formation of a 2D B-mode image. The image is built p line by line as the beam is stepped along the transducer array.*

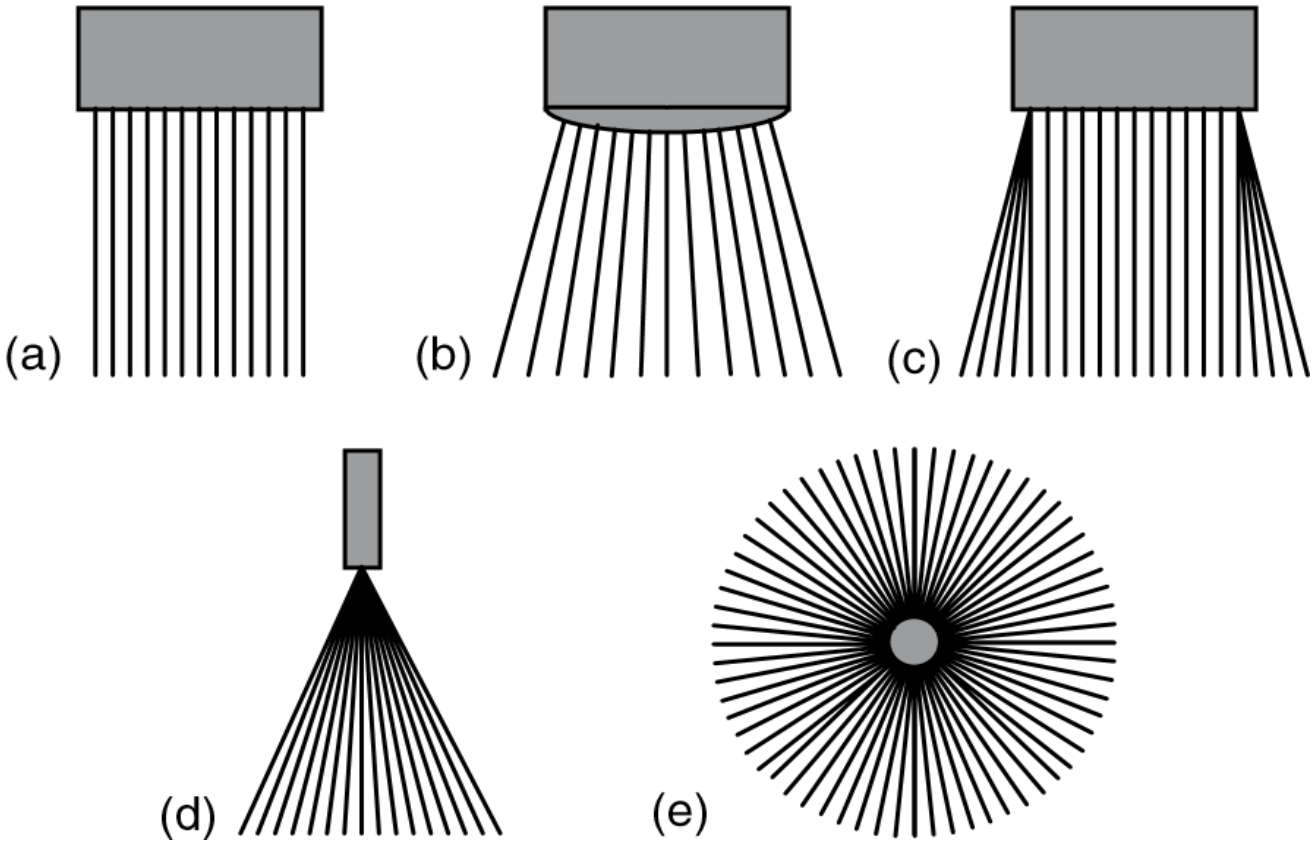


*Figure 1:5 Scan line arrangements for the most common B-mode formats*

There are many B-mode formats. These are (a) linear, (b) curvilinear, (c) trapezoidal, (d) sector and (e) radial.

An overview of the image acquisition using ultrasound is presented in Figure 1-6 and Figure 1-7.

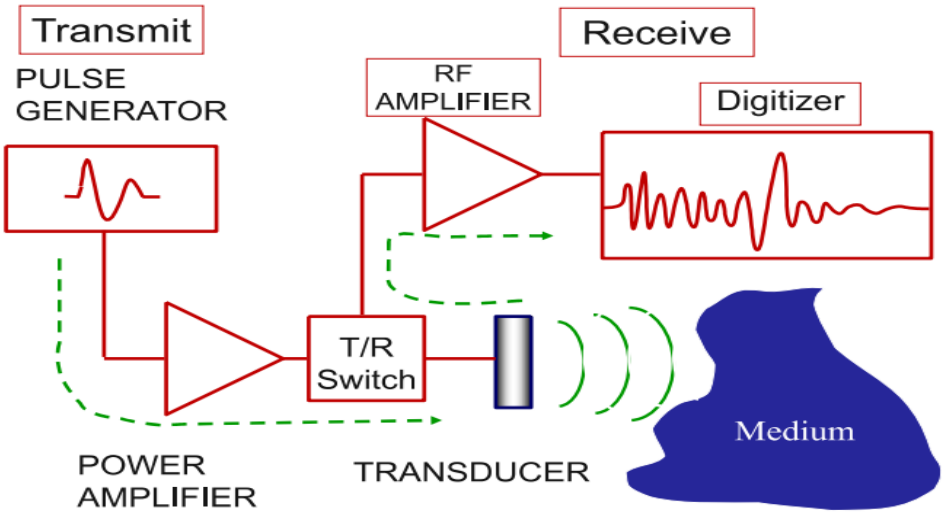


*Figure 1:6 Basic Pulse-Echo Ultrasound System (Image Courtesy: Dr. S. Kaisar Alam, Rutgers University, NJ, USA)*

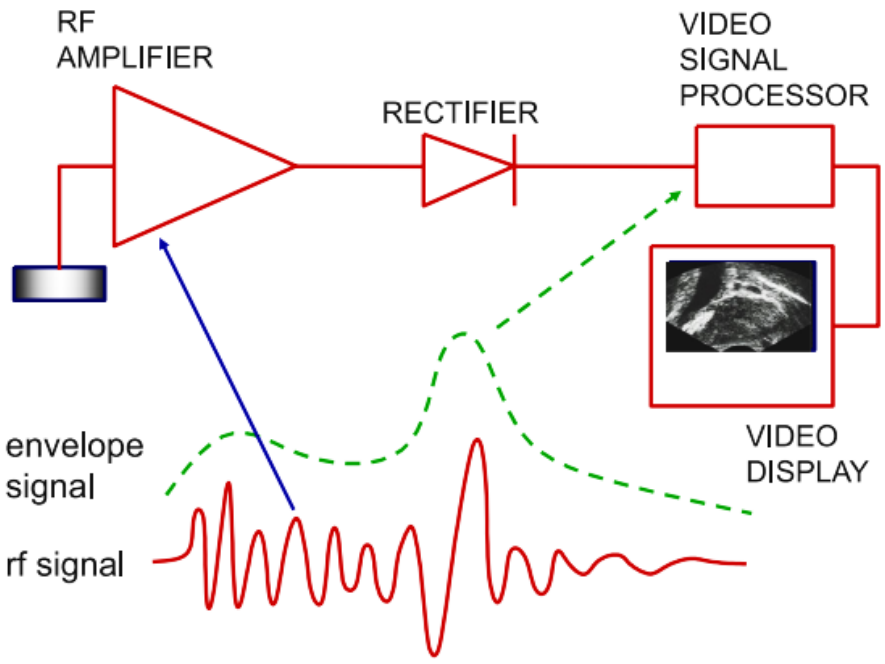


*Figure 1:7 B-mode image formation (Image Courtesy: Dr. S. Kaisar Alam, Rutgers University, NJ, USA)*

### 1.2.7 Challenges in Ultrasound image interpretation:

Artifacts are presentations on the display which are added or omitted, or are of improper location, brightness, shape, and size compared with the true anatomical features. Some artifacts are useful in interpretation, while others may cause confusion and error. A good understanding of artifacts, why they arise and how to deal with them when they occur, is important in the practice of Ultrasound. Failure to recognize imaging artifacts may lead to complications, including incorrect needle placement or deposition of local anesthetic in the wrong location or hazardous areas. Artifacts are commonly observed during ultrasound-guided nerve blocks and may be related either to the tissues, the block needle, or both. The most common artifacts observed during US are either acoustic or anatomic. Acoustic artifacts are usually the result of incorrect assumptions during processing by the instrumentation. Anatomic artifacts are tissue structures which resemble the target nerve. These errors are also referred to as 'pitfall errors'.

### 1.2.8 Ultrasound imaging in Breast cancer detection:

Ultrasonography (US) is currently considered the first-line examination in the detection and characterization of breast lesions including the evaluation of breast cancer [11]. Yet only few single-center cohort studies analyzing breast US in the framework of screening could be identified. In spite of mammography consider as the primary method for screening especially the noteworthy ability of micro calcifications detection. US is good in mass or mass- like lesion detection, especially in the dense breast population that proved by the study of ACRIN 6666 [11].

Some 35–45% of nonpalpable cancers are detected as micro calcifications in mammographic studies. These micro calcifications can sometimes be visualized by

modern ultrasound (US) equipment, but cannot be reliably identified as such without knowledge of mammography [12]. Palpable mass is not equal to advanced cancer and DCIS (Ductal carcinoma in situ) may present as a palpable mass. In pathologic nipple discharge, for detection of intraductal mass or hypoechoic irregularly subareolar mass, and differentiating between intraductal papillomas and carcinoma in situ and invasive cancer ultrasound, Ultrasound is a useful diagnostic tool superior to mammography and may be worth including in the routine evaluation. DCIS now accounts for as much as 30% of breast cancers in the general screening population and approximately 5% of breast carcinomas in symptomatic women.

Studies have demonstrated that using US images can discriminate benign and malignant masses with a high accuracy [7]. There is a high rate of false positives in mammography which causes a lot of unnecessary biopsies. In contrast, the accuracy rate of BUS imaging in the diagnosis of simple cysts is much higher [7].

Use of ultrasound can increase over all cancer detection by 17% [8] and reduce the number of unnecessary biopsies by 40% which can save as much as $1 billion per year in the United States alone.

Breast ultrasound (BUS) imaging is better than mammography for various reasons, like it requires no radiation, ultrasound examination is more convenient and safer than mammography for patients and radiologists in daily clinical practice and it is also cheaper.

That’s why, day by day Ultrasound is becoming a major tool for detecting breast cancer.

## 1.3 Thesis Objectives

The main aim of this thesis work is to facilitate diagnosis of breast cancer globally. The context of this thesis work is, “An approach to improve breast cancer detection by using various strain estimation methods and image segmentation on breast ultrasound (BUS) Images”. This includes qualitative analysis by strain estimation method like 1D (gradient) method, 1.5D, 2D, adaptive stretching and short-term correlation methods and then finally accurate breast lesion segmentation in US images.

Therefore, the objective of this thesis work was to develop more robust, accurate and automatic breast lesion depiction and segmentation. This work is supposed to help physicians in commenting on the nature of the breast lesion. We hope that the outcome of this thesis will help in breast cancer treatment in future.

## 1.4 Thesis Organization

The thesis is organized in the following way:

Chapter 2 (Background) presents the literature review and state-of-art situation of problem

Chapter 3 Speckle and Noise Reduction using various filters

Chapter 4 Various Strain Estimation methods from Breast Ultrasound (BUS) data

Chapter 5 Working of adaptive stretching along with 2D strain estimation method

Chapter 6 Breast Lesion Segmentation

Chapter 7 Conclusion and Future scope of research:

# 2 Background

## 2.1 Related Work

There have been many researches already done in this field. This field covers the vast area of Coded Excitation, Elasticity Imaging and Motion Estimation, Electrical Impedance, Image segmentation, Quantitative Ultrasound, Seed Imaging, Speckles and Speckle Reduction, Texture Analysis, Ultrasound Attenuation, Wavelets etc. [13],[14]

There are many types of Elasticity Imaging. Among them Sonoelasticity & Strain estimation are main. Sonoelasticity imaging technique consists of the vibration amplitude pattern of the shear waves in the tissue under investigation is detected and a corresponding color image (similar to color Doppler display) is superimposed on the conventional grayscale image. A theory of sonoelasticity imaging was developed and in vitro results on excised human prostate were promising.[15],[16]

Strain estimation is done by applying compression to the tissue and then calculate the difference between the pre-compression post-compression data. There are many ways of calculating the strain, like using correlation, adaptive stretching etc.[17],[18]

Several papers have discussed automatic segmentation of known anatomic structures from medical images. Many of these algorithms rely on a priori shape information of the organ or structure of interest to segment it out, a priori shape information was used to

segment ventricular structures in echocardiograms.[19] The problem of segmenting ultrasonic breast lesions using these methods is the variance of their shape and the fact that often lesion margins are poorly defined. Region-based methods, e.g., fuzzy connectedness,[20] use some homogeneity statistics coupled with low-level image features like intensity, texture, histograms, and gradient to assign pixels to objects. If two pixels are similar in value and connected to each other in some sense, they are assigned to the same object. These approaches, however, do not consider any shape information.

The problem of applying these techniques to finding ultrasonic breast lesions is that they cannot deal with shadowing artifacts. Posterior acoustic shadowing is a common artifact in ultrasound images. It appears as a dark area below the tumor. Pixels within this area have an intensity and texture similar to points within the tumor region and, consequently, will be classified as belonging to the lesion.

Some researchers have proposed hybrid segmentation techniques. These approaches seek to exploit the local neighborhood information of region-based techniques, and the shape and higher-level information of boundary-based techniques. However, without manual intervention these hybrid techniques cannot distinguish other structures in the sonogram, e.g. subcutaneous fat, coopers ligaments, and glandular tissue, from the true lesion. [21] [22]

## 2.2 Overview of Proposed Method:

Overview of the proposed method can be broken into three steps. Firstly, strain estimation and finding out the lesion, then segmentation and lastly qualitative analysis. The flow chart of the proposed method is presented in Figure 2-1

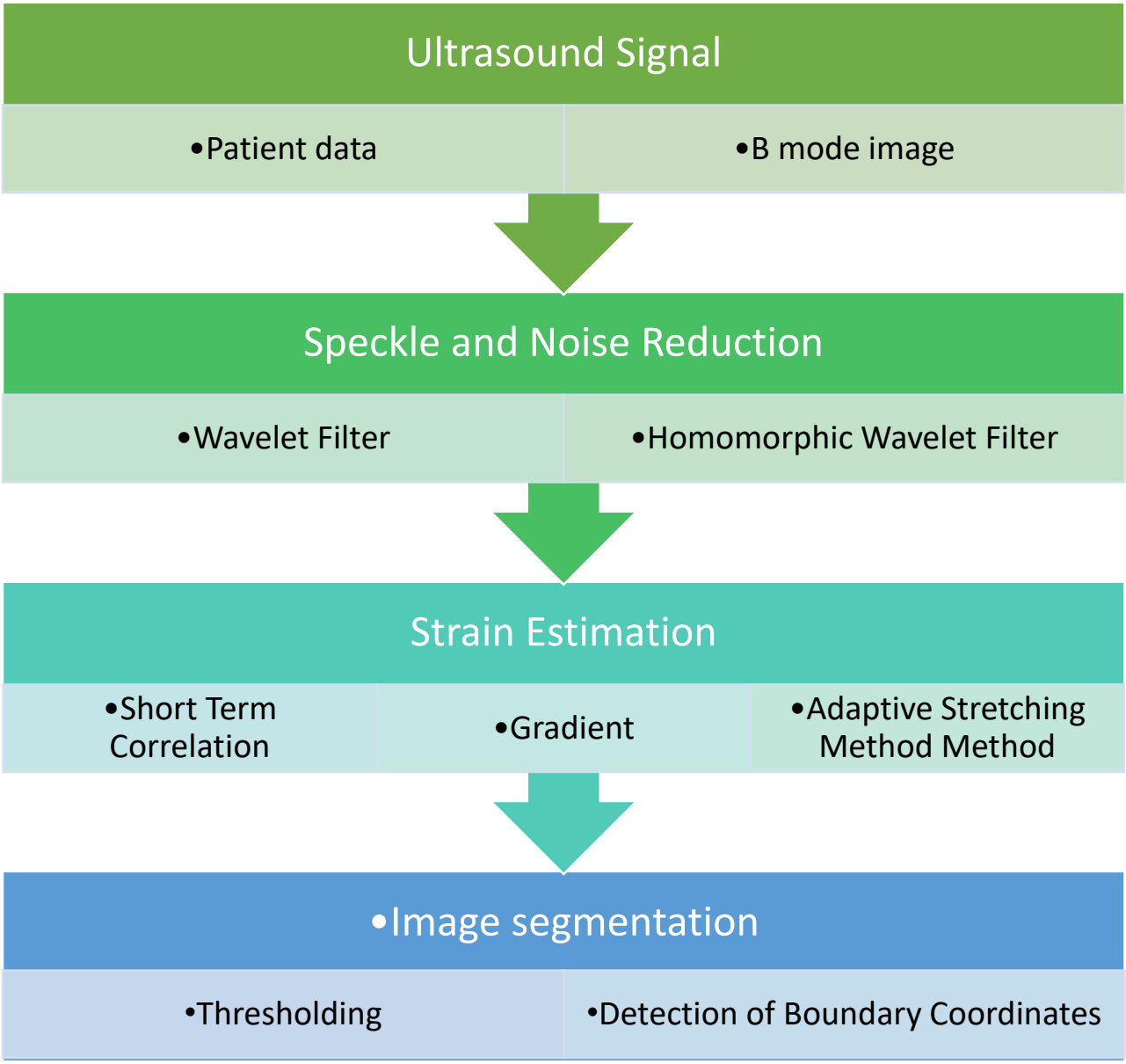

# 3 Speckle and Noise Reduction using various filters

## 3.1 Introduction:

Medical images are usually corrupted by noise in its acquisition and Transmission. The main objective of Image denoising techniques is necessary to remove such noises while retaining as much as possible the important signal features [23].

In medical image processing, image denoising has become a very essential exercise all through the diagnosing process.

Ultrasonic imaging is a widely used medical imaging procedure because it is economical, comparatively safe, transferable, and adaptable. Though, one of its main shortcomings is the poor quality of images, which are affected by speckle noise. The existence of speckle is unattractive since it degrades image quality and it affects the tasks of individual interpretation and diagnosis. Accordingly, speckle filtering is a central pre-processing step for feature extraction, analysis, and recognition from medical imagery measurements [23].

In certain cases, for instance in Ultrasound images, the noise can restrain information which is valuable for the general practitioner. Consequently, medical images are very inconsistent, and it is crucial to operate case to case. An appropriate method for speckle reduction is one which enhances the signal to noise ratio while conserving the edges and lines in the image [24].

## 3.2 Application techniques:

- Applied on the strain image directly.
- Applied on displacement matrix and then found out strain.
- Applied directly on RF data and then calculated strain.
- Applied on the envelope of the RF data and found out the strain.
- Applied on the B mode image.

Among these five techniques the last two showed promising results.

## 3.3 Filters used:

Some basic filter used initially

- Median Filter (window size 5)
- Ideal Filter (cutoff frequency 30)
- Butterworth Filter (cutoff frequency 30)

### 3.3.1 MEDIAN FILTER:

The median filter is a nonlinear digital filtering technique, often used to remove noise from an image or signal. Such noise reduction is a typical pre-processing step to improve the results of later processing (for example, edge detection on an image).

The main idea of the median filter is to run through the signal entry by entry, replacing each entry with the median of neighboring entries. The pattern of neighbors is called the "window", which slides, entry by entry, over the entire signal.

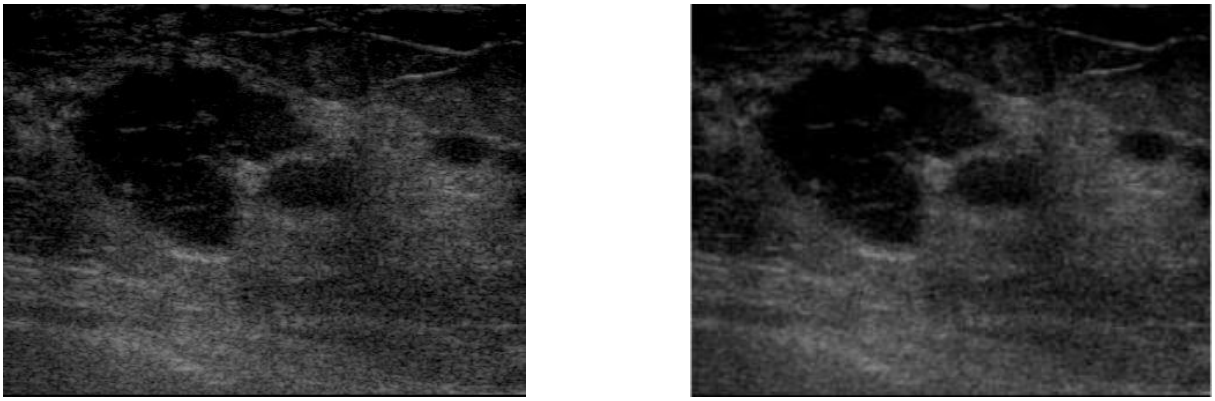

( a ) ( b )

*Figure 3:1 Median filter on BUS: ( a ) Unfiltered image ( b ) Filtered image*

### 3.3.2 IDEAL FILTER:

An ideal low-pass filter completely eliminates all frequencies above the cutoff frequency while passing those below unchanged; its frequency response is a rectangular function and is a brick-wal filter.

An ideal high-pass filter completely eliminates all frequencies below the cutoff frequency while passing those above unchanged; its frequency response is a rectangular function and is a brick-wal filter.

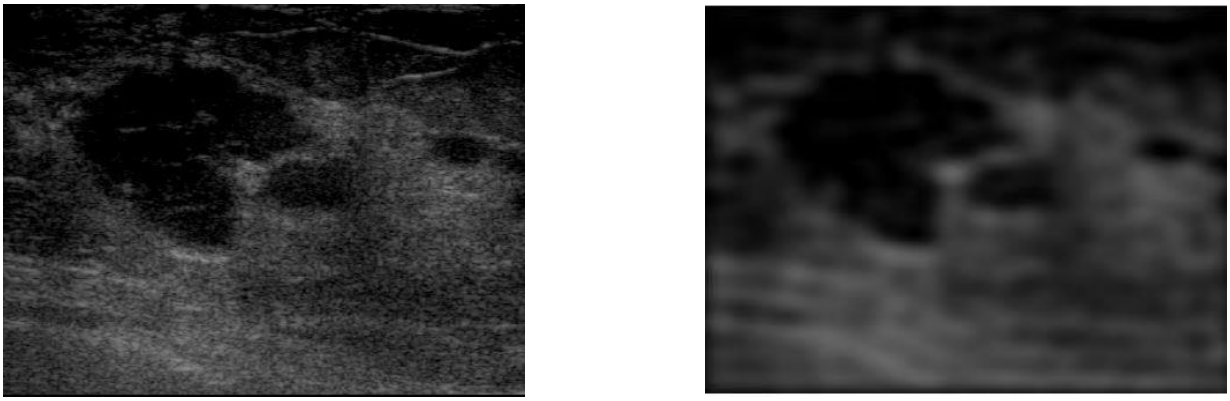

( a ) ( b )

*Figure 3:2 Ideal low pass filter on BUS: ( a ) Unfiltered image ( b ) Filtered image*

### 3.3.3 BUTTERWORTH FILTER:

The Butterworth filter is a type of signal processing filter designed to have a frequency response as flat as possible in the pass band. It is also referred to as a maximally flat magnitude filter.

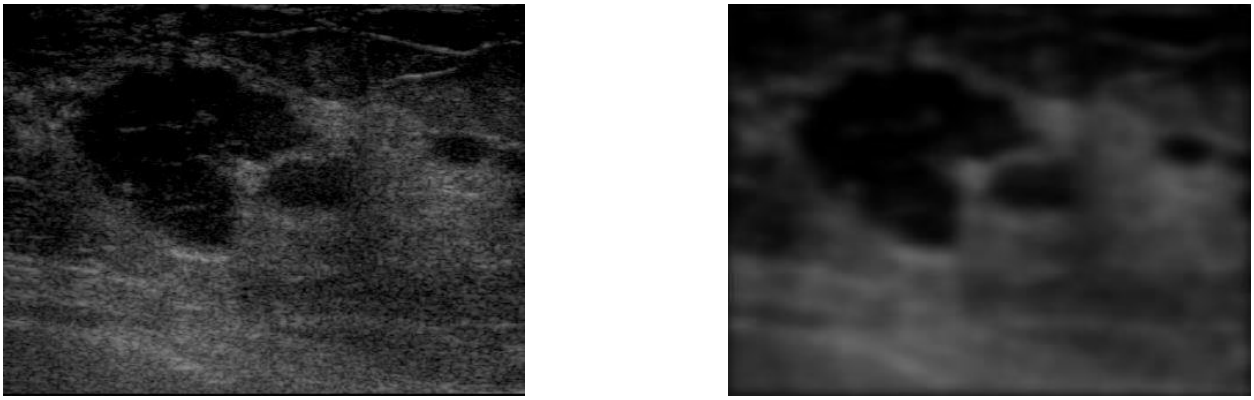

( a ) ( b )

*Figure 3:3 Butterworth filter on BUS: ( a ) Unfiltered image ( b ) Filtered image*

The above mentioned filters did not work well in reducing noise because these filters need a specific cut-off frequency for operation, but in our case of Ultrasound imaging the specific frequency range of noise is unknown. In this case filters having inherent characteristics of choosing threshold cut off frequencies automatically are of great interest.

## 3.4 WAVELET FILTER:

A wavelet is a wave-like oscillation with an amplitude that begins at zero, increases, and then decreases back to zero. It can typically be visualized as a "brief oscillation" like one recorded by a seismograph or heart monitor. Generally, wavelets are intentionally crafted to have specific properties that make them useful for signal processing.

The main advantage of wavelet basis is that they despite having irregular shape are able to perfectly reconstruct functions with linear and higher order polynomial shapes, such as, rectangle, triangle, 2nd order polynomials, etc. Note that Fourier basis fail to do so, as in case of famous example of rectangle function at the edges. As a result, wavelets are able to denoise the particular signals far better than conventional filters that are based on Fourier transform design and that do not follow the algebraic rules obeyed by the wavelets. Wavelet transform can be used to set automatic threshold values. In the past few years, researchers in applied mathematics and signal processing have developed powerful wavelet methods for the multiscale representation and analysis of signals [25]-[27].

One widespread method exploited for speckle reduction is wavelet shrinkage. When multiplicative contamination is concerned; multiscale methods engage a preprocessing step consisting of a logarithmic transform to separate the noise from the original image. Then different wavelet shrinkage approaches are employed. The well-known technique of wavelet shrinkage Universal threshold (Visu shrink) that over-smooth images [28], [29]. This threshold was later improved by minimizing Stein’s unbiased risk estimator [30].

### 3.4.1 Wavelet properties:

- ❑ Scaling

Scaling refers to the process of shrinking or stretching the signal in time.

Scaling is inversely proportional to frequency.

- ❑ Shifting

Shifting a wavelet means delaying or advancing the onset of the wavelet along the length of the signal.

### 3.4.2 Working principle of wavelet filter:

This filter preserves both the high and low frequency components. Wavelet filter uses both low pass and high pass filters at different levels, which leads to different level decomposition. On each level the signal is subsampled by 2, as Nyquist theorem states that original signal can be retrieved from the intermediate signal only if the sampling frequency is not less than twice the frequency of the original signal. After the next level decomposition, the output extracted are the following four parameters:

1) Approximate Image of the original matrix
2) Vertical detail
3) Horizontal detail
4) Diagonal detail

Then the three detailed parameters are compared with zero, and if their values are close to zero it neglects all the detailed values. As a result, the approximate matrix can be considered as the output of filter containing both high and low frequency components, where the unwanted noise gets diminished.

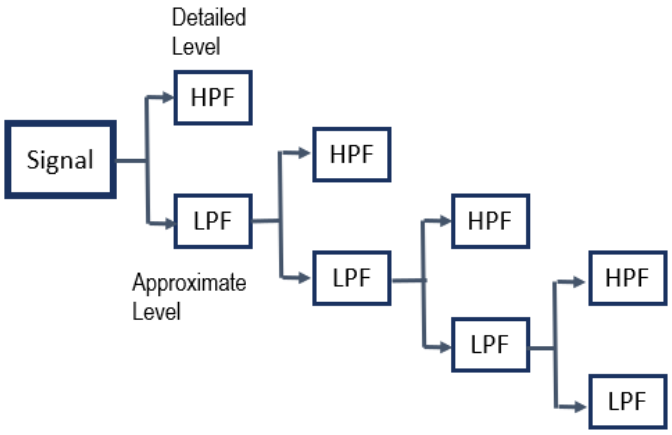


### 3.4.3 Results:

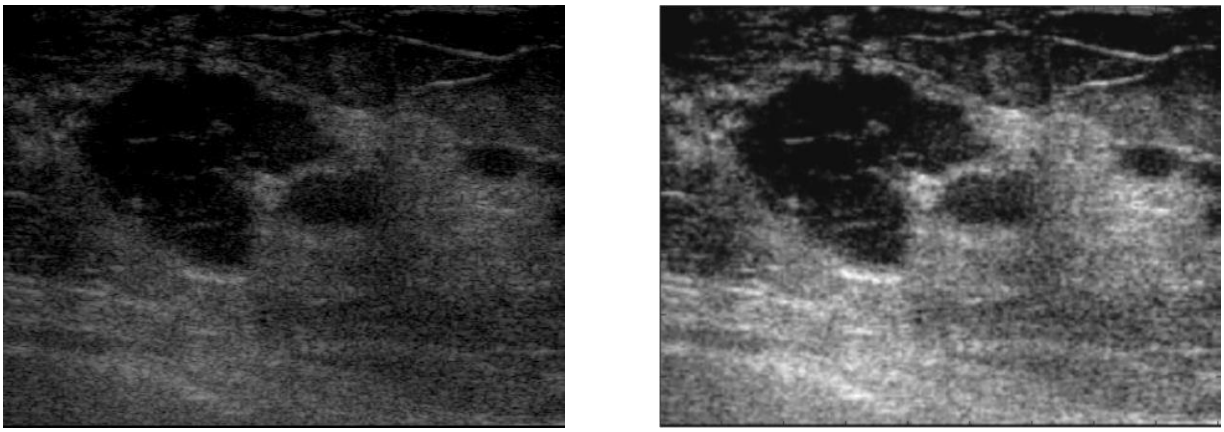

( a ) ( b )

*Figure 3:4 Wavelet filter on BUS, Case 1: ( a ) Unfiltered image ( b ) Filtered image*

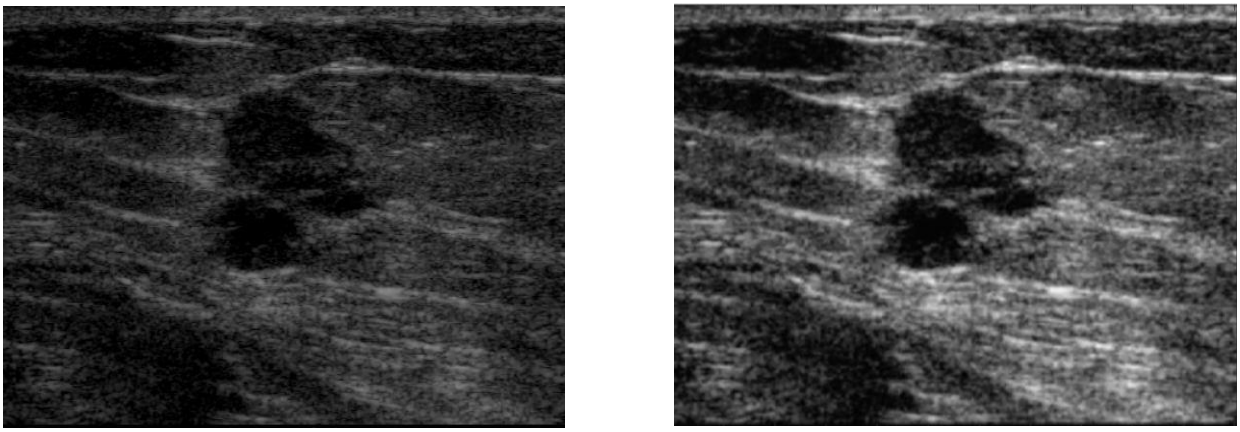

( a ) ( b )

*Figure 3:5 Wavelet filter on BUS, Case 2: ( a ) Unfiltered image ( b ) Filtered image*

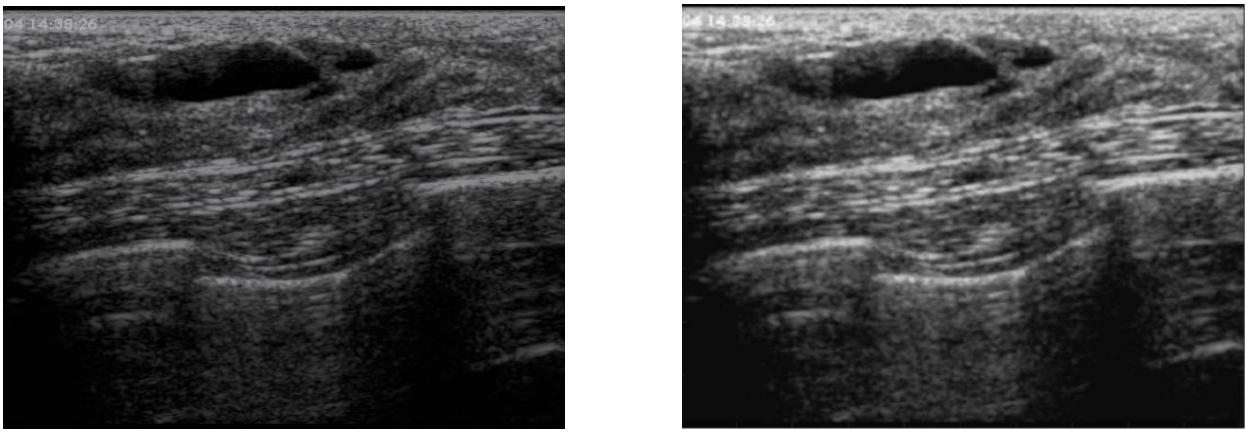

( a ) ( b )

*Figure 3:6 Wavelet filter on BUS, Case 3: ( a ) Unfiltered image ( b ) Filtered image*

( a )

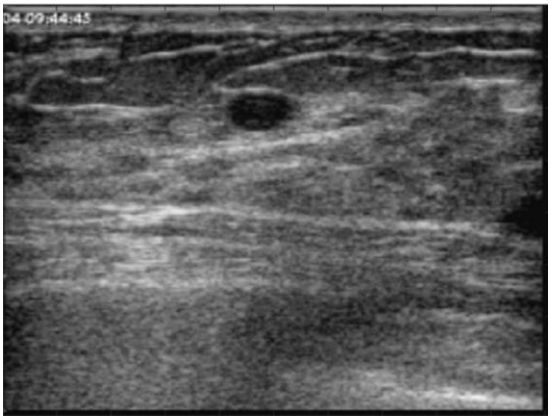

( b )

*Figure 3:7 Wavelet filter on BUS, Case 4: ( a ) Unfiltered image ( b ) Filtered image*

The results suggest that after filtering the difference between the inside and outside of the lesion increases. The boundary of the lesions are easily visible and helps in image segmentation and post processing techniques.

## 3.5 HOMOMORPHIC WAVELET FILTERING:

Homomorphic filtering is a generalized technique for signal and image processing, involving a nonlinear mapping to a different domain in which linear filter techniques are applied, followed by mapping back to the original domain.

Homomorphic wavelet filter is a logarithmic filter used to remove multiplicative noise components.

- Used to remove shading effect from an image due to uneven illumination.
- The noise in a signal is most of the times present in an additive manner
- But it can also be present in a multiplied manner.
- $F(x,y) = i(x,y)\, r(x,y)$

- To get rid of these we can take the signal in logarithm and then pass it through wavelet filter.

### 3.5.1 Results:

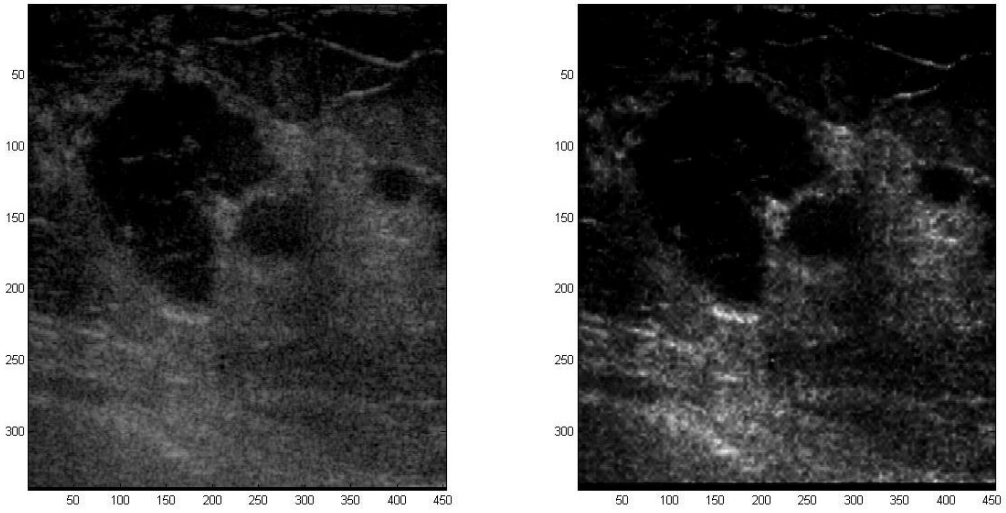


( a ) ( b )

*Figure 3:8 Homomorphic Wavelet filter on BUS : ( a ) Unfiltered image ( b ) Filtered image*

The results for homomorphic wavelet filter were not as expected, the boundary of the lesion becomes imprecise.

So, as we sum it up we can conclude that, wavelet filter performs the best in our BUS data set.

# 4 Various Strain Estimation methods from Breast Ultrasound data

## 4.1 1D Shear elastography probe [31]

The 1D transient elastography probe was first developed at the Institut Langevin in 1995 by Catheline et al. [32]. It consists of generating a transient impulse (little shock) on the medium and recording the shear wave that propagates within the medium by using an ultrasound transducer (Fig: 4.1).

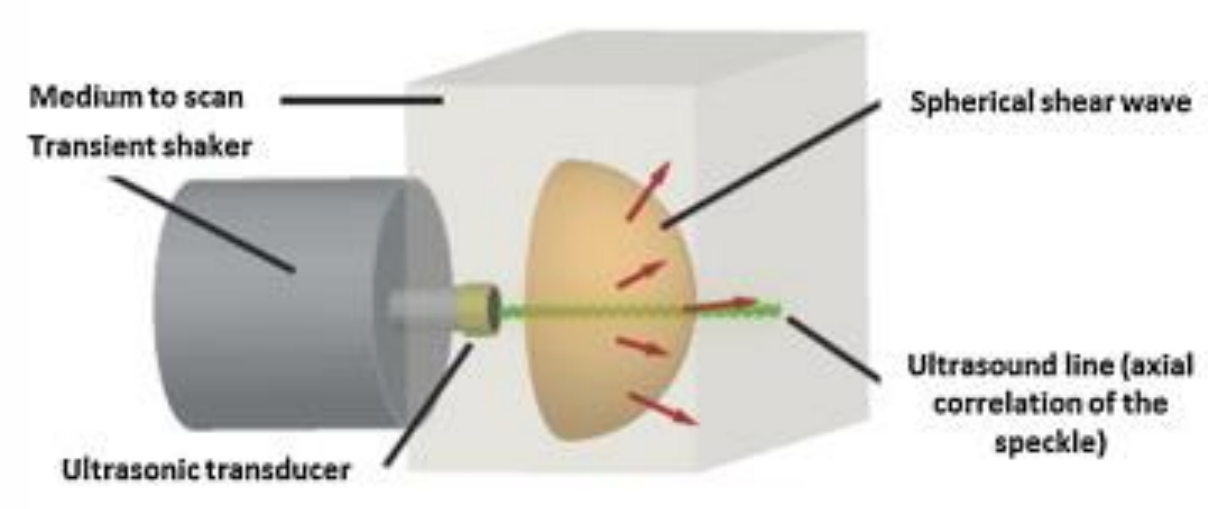


*Figure 4:1 transient elastography probe*

The vibrator gives a low frequency pulse (adjustable from 10 Hz to 500 Hz) in the medium, creating, among others, a shear wave. The ultrasound transducer, which is placed on the vibrator, thus allows following, by axial intercorrelation of the ultrasound speckle and more than one thousand times per second, the propagation of the shear wave depending on the depth over time. We can then deduce the speed of the shear wave and thus the Young's modulus of the medium.

First, the front face of the transducer acting as a piston gives a slight mechanical impulse on the surface of medium, which generates a spherical compression wave as well as a spherical shear wave [33]. The displacement generated, which is a function of depth and of time, is thus estimated by correlations of retro-diffused echoes (via ultrasound speckle) recorded at a framerate higher than one thousand time per second with a mono-dimensional ultrasound transducer (5 MHz) (fig: 4.2).

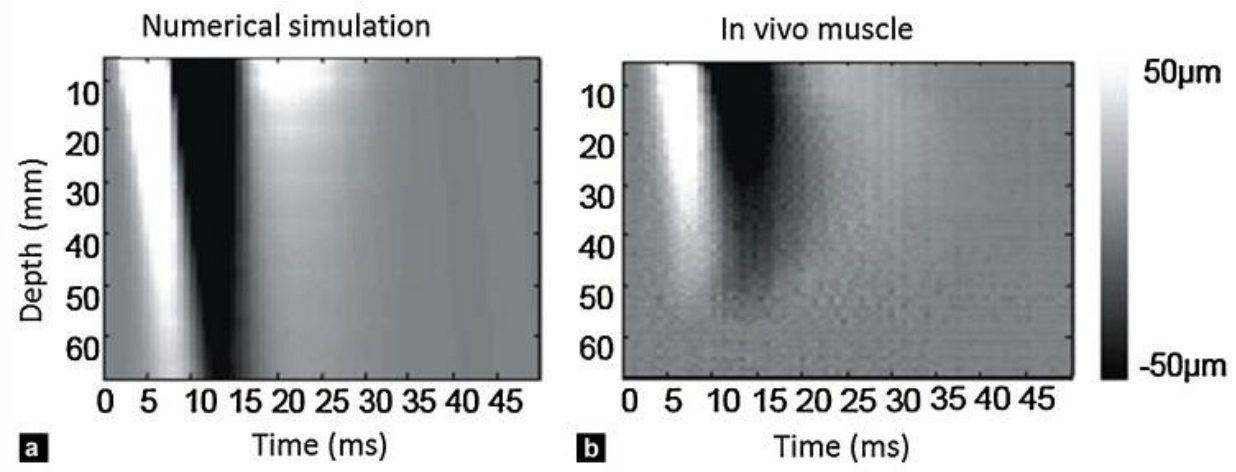


*Figure 4:2 Output from the probe*

Comparison between the (a) numerical simulation of the time/depth profile and the (b) Time/depth profile in a muscle in vivo. The extraction of the slope allows to work back to the speed of the shear wave and thus the Young's modulus of the medium.

Finally, by measuring the phase for each depth, we extract the phase speed of the shear wave at the central frequency, leading to an estimation of Young's modulus by considering the medium to be homogeneous and non-viscous. This approach, which was initially designed for quality control in the food industry, was then applied to the medical field [34] and developed for the measurement of other mechanical parameters, such as anisotropy, viscosity or elastic non-linearity [35], [36], [37].

## 4.2 1D strain estimation (gradient) method:

When an elastic medium, such as tissue, is compressed by a constant uniaxial stress, all points in the medium experience a resulting level of longitudinal strain whose principal components are along the axis of compression. If one or more of the tissue elements has a different stiffness parameter than the others, the level of strain in that element will generally be higher or lower; a harder tissue element will generally experience less strain than a softer one. The longitudinal axial strain is estimated in one dimension from the analysis of ultrasonic signals obtained from standard medical ultrasound diagnostic equipment. This is accomplished by acquiring a set of digitized radio-frequency (RF) echo lines from the tissue which is being recorded as ".eye" file and is then post processed using 1D strain estimator algorithm. There would be two corresponding pre and post compression data matrix.

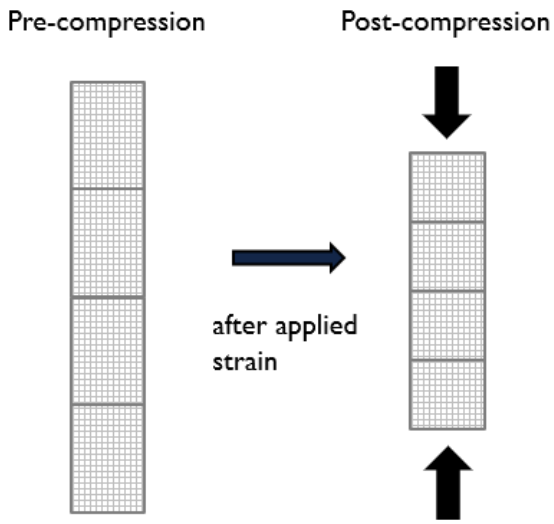


*Figure 4:3 Pre & Post Compressed window*

The local longitudinal strain is estimated as:

$$e_{11.local} = \frac{(t_{1b} - t_{1a}) - (t_{2b} - t_{2a})}{t_{1b} - t_{1a}}$$

Where t1a is the arrival time of the pre-compression echo from the proximal window, t1b is the arrival time of the pre-compression echo from the distal window, t2a is the arrival time of the post-compression echo from the proximal window and t2b is the arrival time of the post compression echo from the distal window [38].

Flowchart for 1D strain estimation:

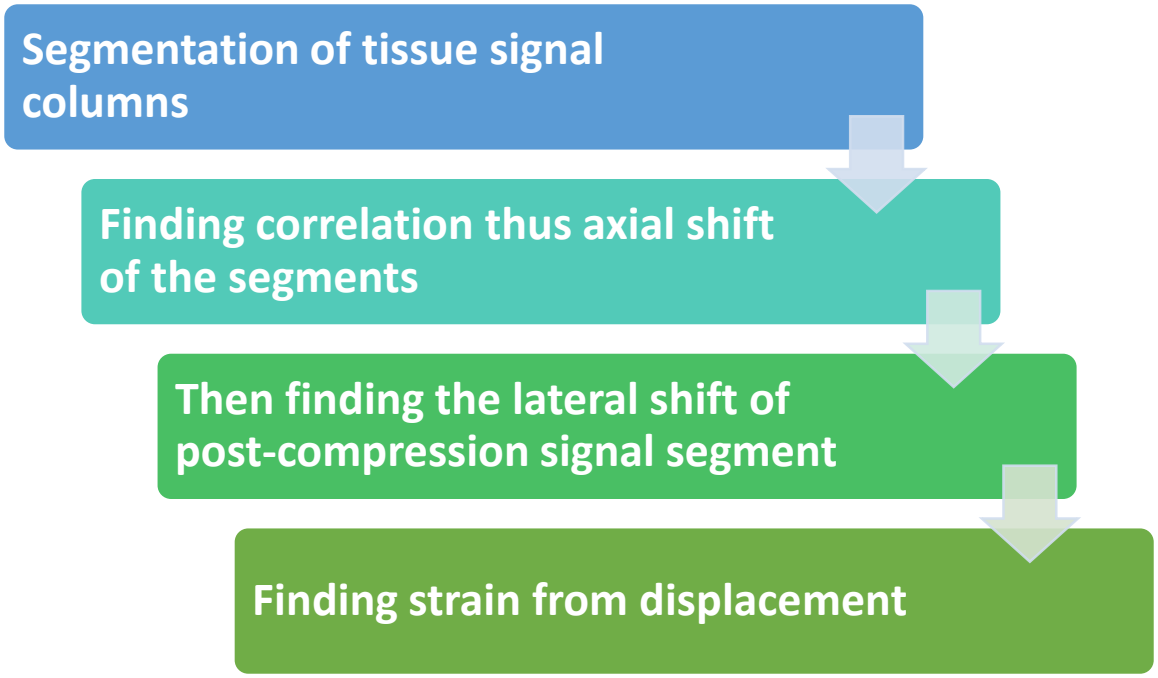


Initially, the pre-compression echo signals were segmented into overlapping 1D windows. Using the above equation, correlation of the axial shift elements are being calculated using the pre and post compression data matrix. A segment from pre-compression $i^{th}$ column was correlated with the corresponding segments of $(i_n)^{th}$ to $(i+n)^{th}$ post-compression column.

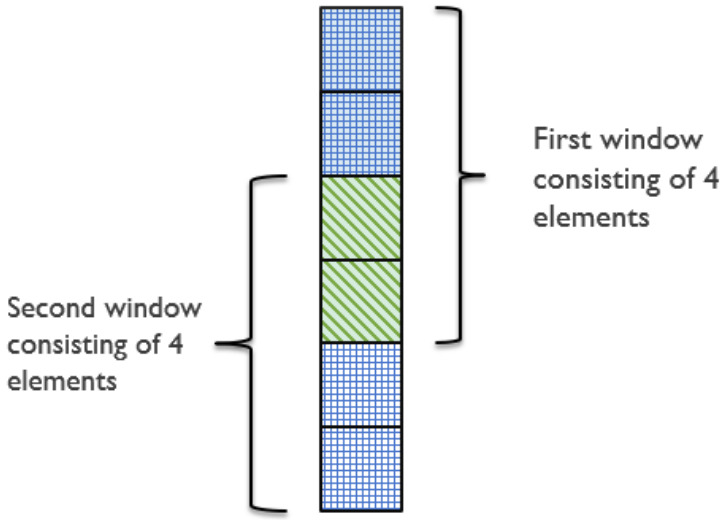


*Figure 4:4 Overlapping Windows*

For each post compression column, the maximum correlation was calculated, yielding 2n+1 maximum correlation value. Then, we calculated which of these 2n+1 correlation value is the highest; in other words, which axial segment of the post compression data had the highest correlation with the pre-compression data segment. If the pre-compression data segment ($i^{th}$) had the highest correlation with the $(i+k)^{th}$ post compression data line segment, it meant that tissue deformed in such a way that the corresponding post-compression segment had shifted +k columns. Then the axial strain is simply the estimated using axial tissue strains based on the assumption of tissue incompressibility.

Results obtained using 1D strain estimator:

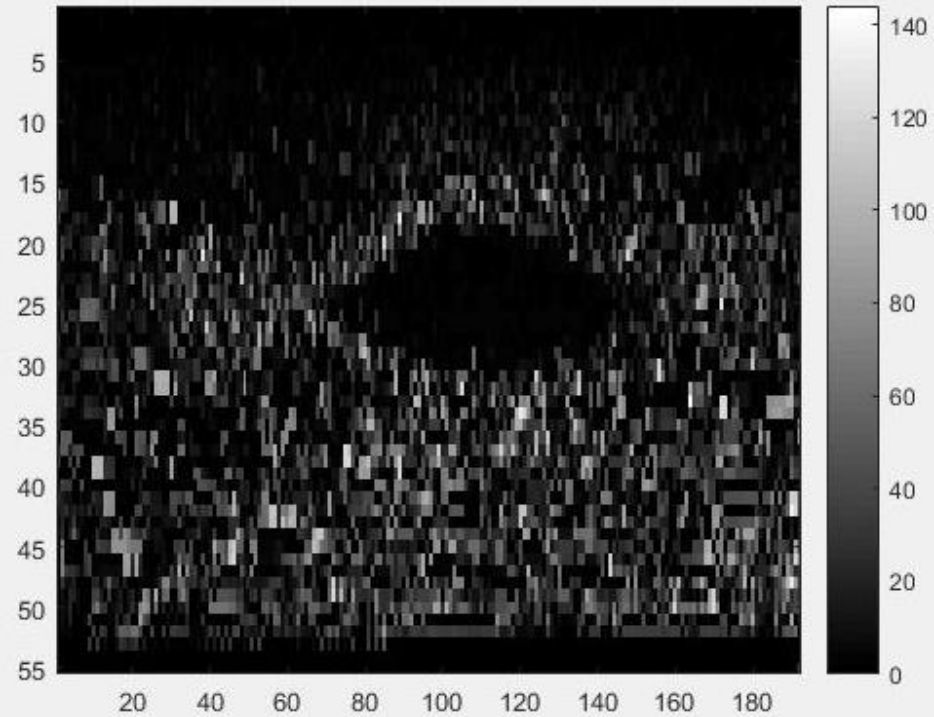


*Figure 4:5 Output from Gradient method*

## 4.3 1.5D strain estimator:

This strain estimator method is a modified version of the basic 1D strain estimator algorithm where the correlation is done both axially and laterally. The gradient (1D) operation introduces significant amount of noise into the strain estimates, especially for small correlation window sizes and/or large overlap between the successive correlation windows.

However, to increase resolution, using a small correlation window size is desirable; moreover, to track rapid changes in elasticity, large window overlap may be used. Because no gradient (1D) operation is associated with this new estimator, it does not suffer from the noise amplification associated with gradient methods. Among the

techniques based on the estimation of tissue strain, elastography is based on estimating the tissue strain using a correlation algorithm.

Whereas another elasticity imaging technique is based on estimating such strain using the phase information. In elastography, the local tissue displacements are estimated from the time delays between gated pre- and post-compression echo signals, whose axial gradient is then computed to estimate the local strain. [39] which leads to the detection of the shape of the lesion.

Below is the flowchart for 1.5D Strain estimation method:

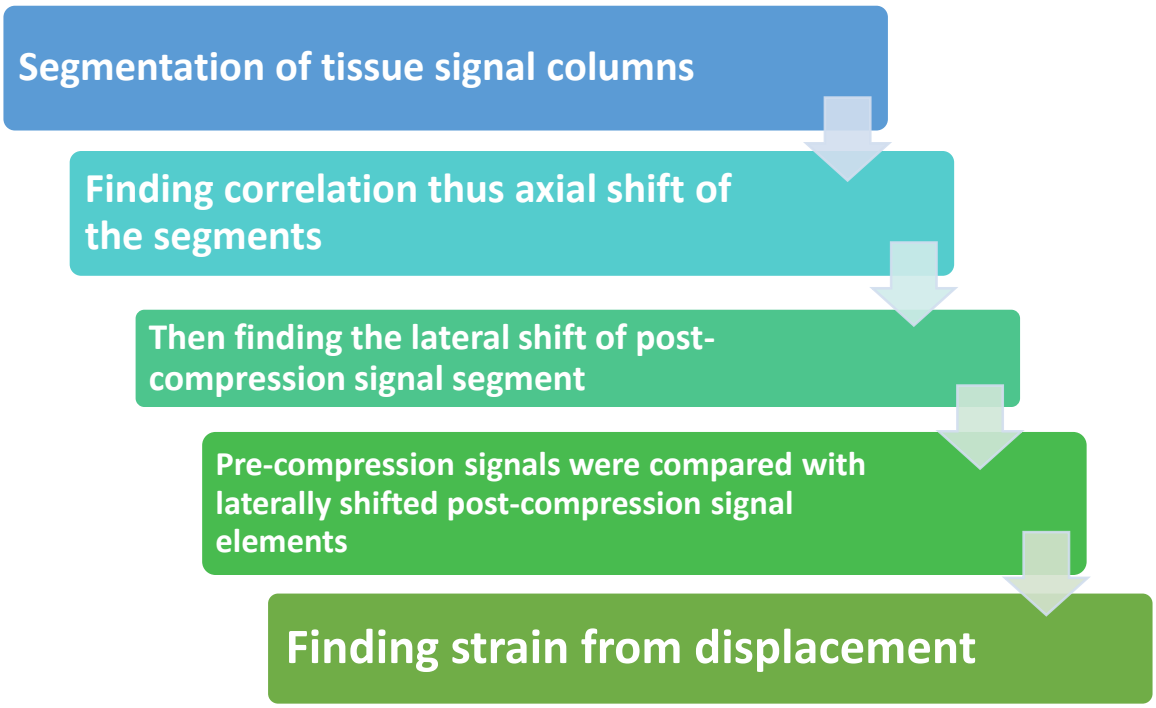

Here is an illustration of the lateral shifting of compressed breast tissue:

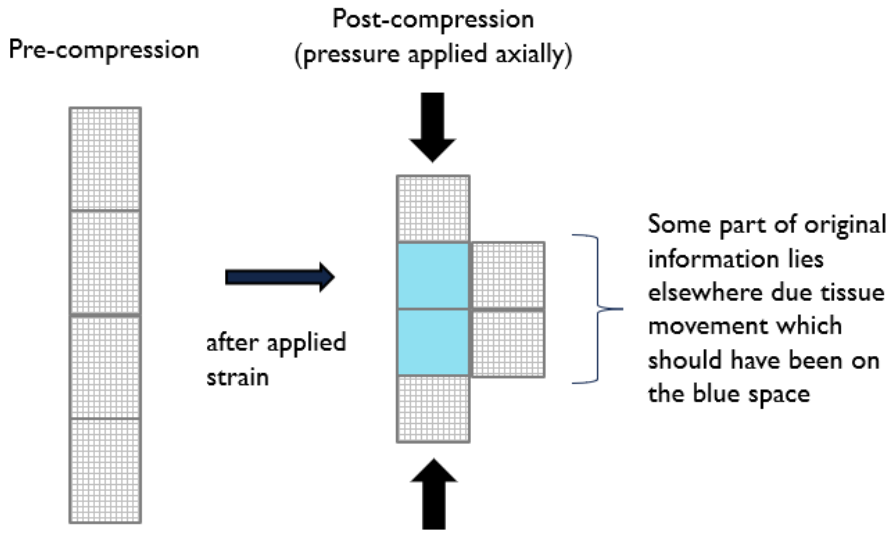


*Figure 4:6 Lateral shifting windows*

When pressure is applied, different part of tissues deforms differently. This happens more when high pressure or stress is applied. As a result, different tissue part may move laterally in different directions and the segments of the pre-compression signal won't correspond to post compression signal in the exact position.

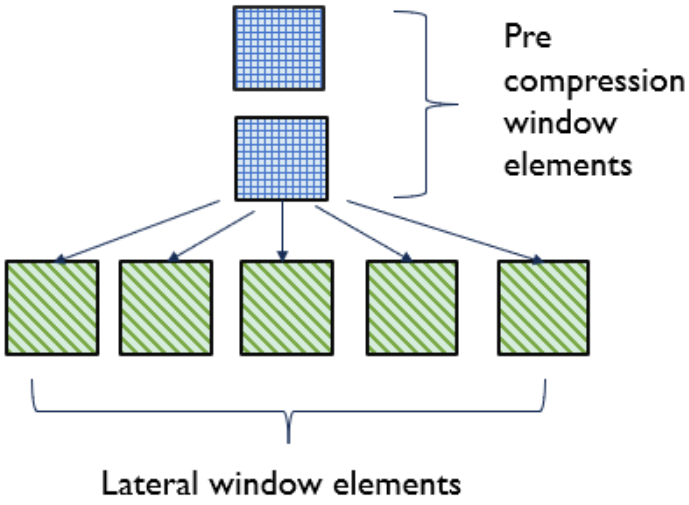


*Figure 4:7 axially shifted 1.5D window elements*

In the above image, the lateral correlation among pre and post compression elements is shown. In the time domain, the lags (displacements) between the segments of pre- and corresponding segments of post compression signal was determined. First difference between two consecutive displacements gives strain.

The displacement map is computed by sliding the pre and post-compression windows and computing the displacement for each pre-compression window.

Strain= ( i , j )$^{th}$ displacement – ( i+1 , j )$^{th}$ displacement

where, i=row and j=column

The strain map is computed using the above equation.

Moreover, because of the compression of the tissue, the post compression signal is not an exact delayed replica of the recompression signal, resulting in decorrelation that increases with increasing strain. Moreover, in an elastically inhomogeneous tissue, the strains will vary and, thus, the stretching factor will have to be varied at different windows. This is why a global uniform stretching of the entire post compression RF line is not ideal for imaging real tissue.

The elastic properties of soft tissues depend on their molecular building blocks, and on the microscopic and macroscopic structural organization of these blocks [29]. The standard medical practice of soft tissue palpation is based on qualitative assessment of the low frequency stiffness of tissue. Pathological changes are generally correlated with changes in tissue stiffness as well. Many cancers, such as scirrhous carcinoma of the breast, appear as extremely hard nodules [40]. [41]

Results obtained using 1.5D strain estimator:

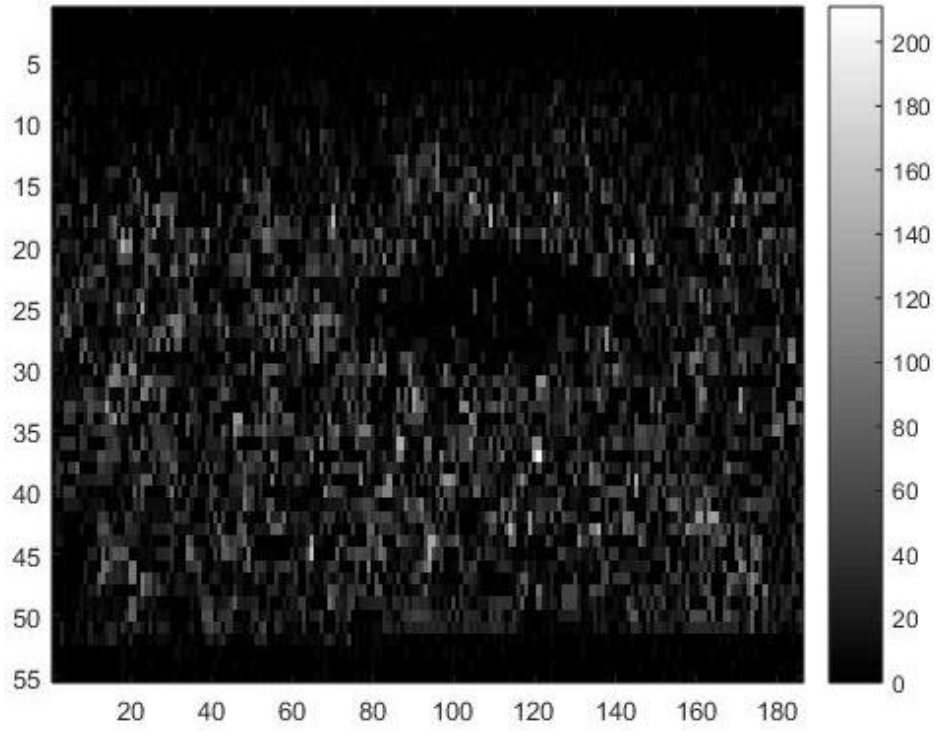


*Figure 4:8 Output from 1.5D*

## 4.4 Short term correlation method:

In this method, the signal columns of tissue samples are further segmented into smaller windows and then correlation is done among those windows. In these cases, the output would be more precise as the speckles in each segment would be reduced.

One static approach or quasi-static to elasticity displacement imaging at the is body to apply a surface creating deformation within the tissue. Induced internal displacements and corresponding strains must then be estimated.

Correlation-based speckle tracking methods are commonly used in ultrasonic elasticity imaging to estimate tissue displacement. If the strain is estimated from the displacement derivative, any displacement noise will be amplified. Therefore,

displacement measurements need to have small error. Induced strain in tissue compounds the problem, however, because it reduces signal coherence leading to increased error in displacements estimated using correlation. [42]

The results demonstrate that high resolution, high SNR strain estimates can be computed using small correlation kernels (on the order of the autocorrelation width of the ultrasound signal) and correlation filtering. The results of these studies, detailed here, will show that a short correlation kernel along with filtering of the correlation functions produces a high strain SNR with high spatial resolution.

A solution to this problem is short term correlation elastography method. In this method, smaller windows are taken within the correlation windows in the pre and post correlation windows.

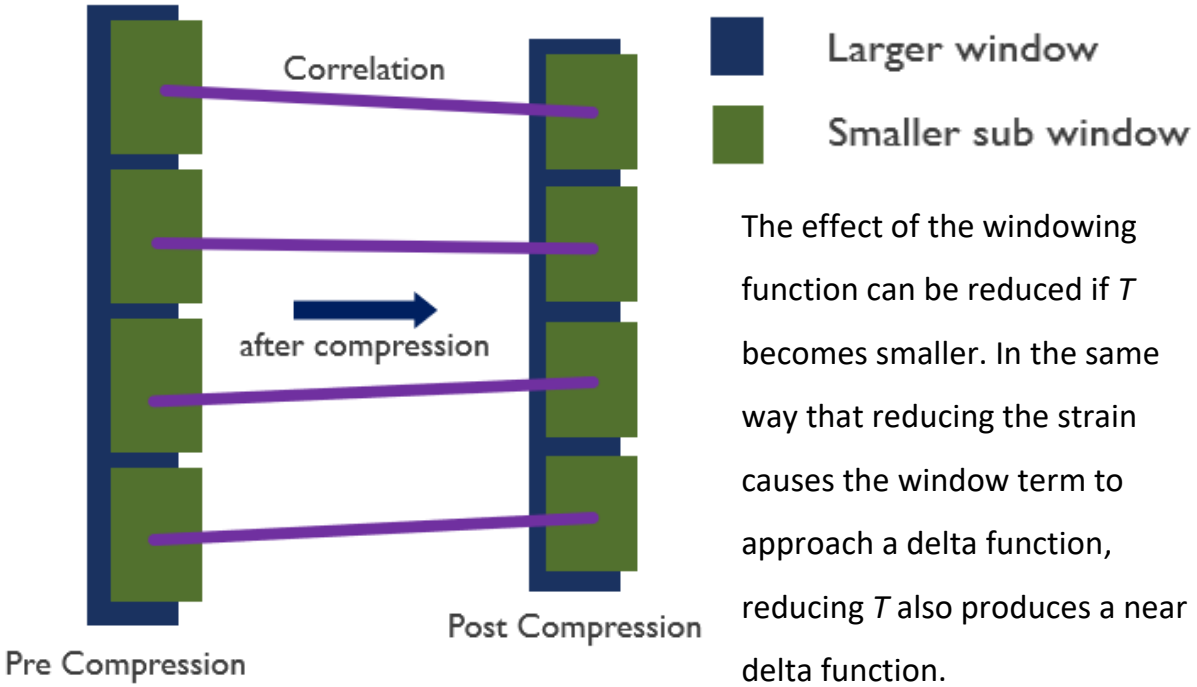


The effect of the windowing function can be reduced if *T* becomes smaller. In the same way that reducing the strain causes the window term to approach a delta function, reducing *T* also produces a near delta function.

*Figure 4:9 Short term correlation (without variable windows)*

Obviously, *T* cannot be reduced to zero because the cross-correlation function will broaden due to other terms. As noted earlier, the variance of the time-delay estimate is reduced if the width of the cross-correlation coefficient function is kept as small as possible. As *T* decreases, the combined effects of the window and distortion terms reduce to a delta function. Consequently, the expected value of the cross-correlation function reduces to a shifted and scaled version of the autocorrelation function

As the window is reduced below the autocorrelation width of the ultrasound pulse, however, the normalization terms fluctuate wildly. These fluctuations can increase the variance in the estimated time delay greatly, and even produce peak hopping errors (see below).

Thus, for a given pulse, p(t), there should be an optimum window length *T* such that the time delay variance is minimized. To explore the effect of window length on time-delay estimates, a simple 1-D deformation simulation was developed.

In the limit of large electronic SNRs, the variance in the time-delay estimate is inversely proportional to the second moment of the signal cross spectrum (i.e. the Fourier transform of the cross-correlation function).

This means, as the correlation peak broadens, the second derivative at the peak decreases in magnitude, and the variance in the estimated time delay increases. To minimize the width of the correlation function near its peak value, and thus minimize time-delay error, the effects of strain must be reduced. One way to do this is to time compand, or temporally stretch, the deformed signal prior to Correlation.

Below is the flowchart for Short term correlation:

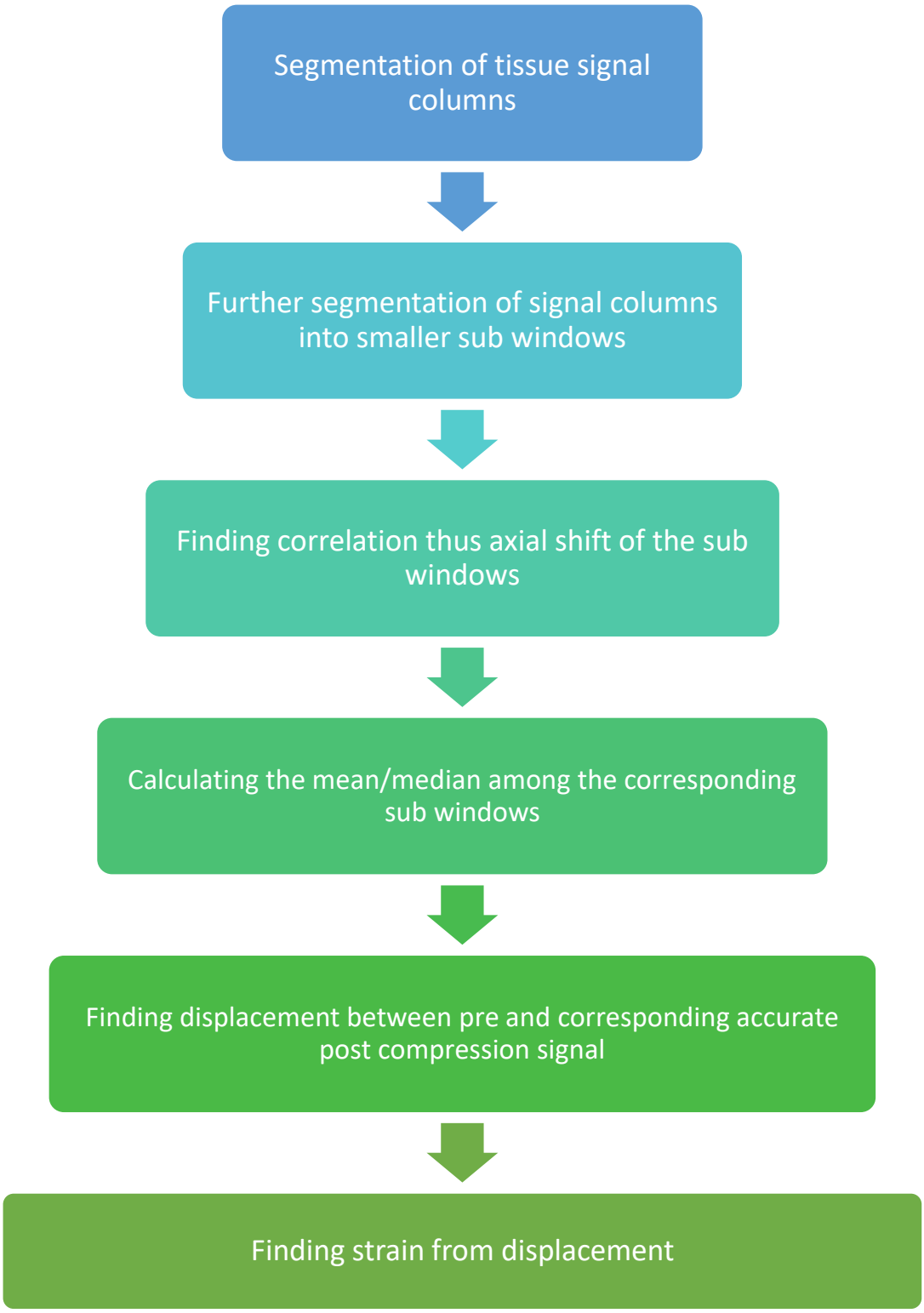

## 4.5 Steps for Short term correlation algorithm:

1. Initially, the pre and post-compression signals were segmented into overlapping primary larger windows.
2. Then again, the pre and post compression window are subdivided into smaller sub windows. Then the corresponding sub windows from pre and post compression windows are correlated.

*Figure 4:10 Correlation matrix*

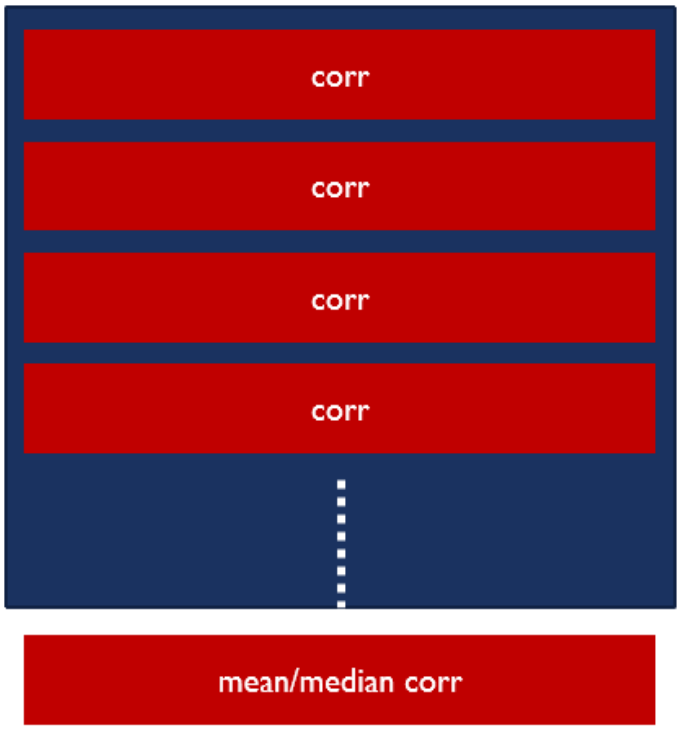


3. After correlation, we get a 2D array of correlation matrix (Fig: 4.10)
4. Then we take the mean/median of corresponding positions of that matrix.
5. Then find out the maximum correlation from that single row of correlation matrix.
6. Finding the corresponding lag for which max correlation occurs.
7. Placing the corresponding maximum lag data in each element of the matrix.
9. Then we plot a diagram based on the displacement matrix. (Fig: 4.11)
10. Strain is calculated from the difference between two consecutive displacements.

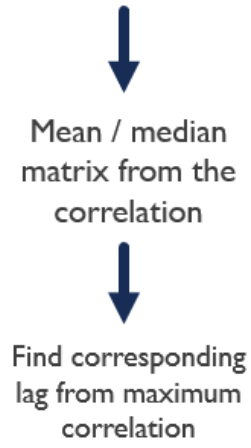

11. The strain map is computed by sliding the pre and post compression windows and computing the displacement for each pre-compression window. Below is the equation for strain map:

**Strain= ( i , j )th displacement – ( i+1 , j )th displacement**

where, i=row and j=column

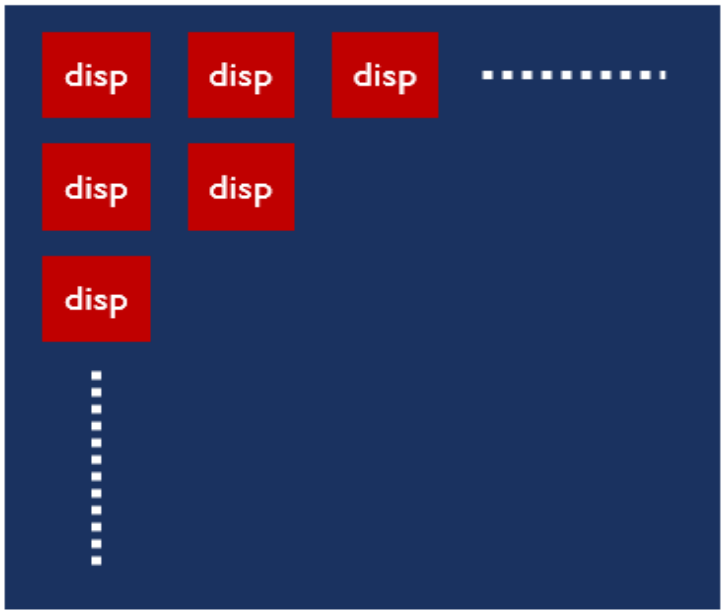


*Figure 4:11 Displacement matrix*

The tradeoffs between window size and variance, the resolution also must be considered. The smaller window gives increased spatial resolution and reduced variance. One of the main advantages of this technique over strain compensation by time companding is its simplicity. Because it is very simple, real-time implementation in hardware has been explored.

Temporal stretching, however, is a computationally intensive algorithm because companding compensation must be searched and the time scaled signal recomputed for

every value of Q tried [43]. These computations are in addition to correlation calculations. The performance of the short-term correlation estimator may be improved using estimates of the strain to compand the correlation function prior to filtering, as in the deskewed short-time correlator by Betz [42].

However, companding adds additional complexity and, from explorations using 1-D simulations, the improvement is slight, even when the strain is constant and known exactly. Additionally, if nonoverlapping windows are used, as by Betz [42], the resolution of the estimate will be reduced. The displacement and strain estimator presented here is not intended to be the final step in producing an elasticity image. The algorithm is designed to produce estimates suitable for elasticity reconstruction. The resulting Young's modulus image removes many of the strain artifacts caused by boundary conditions.

In general, the complete strain tensor is required for elasticity reconstruction, so 2-D tracking provides the necessary lateral displacements in addition to maximizing the correlation. Lateral estimates can be improved greatly prior to reconstruction using incompressibility processing [44],[45].

Additionally, multiple displacement arid strain estimates can be accumulated to larger average strains, improving the strain SNR. This also will allow multiple displacement estimates computed at different average strain values to be combined so low arid high strain regions in the image can be processed at different average strains to optimize strain SNR throughout the image [44].

Another modified version of short-term correlation was also experimented with, where there would be smaller windows within smaller windows of axially shifting windows.

This sort of looping algorithm is said to improve the image resolution and include all the windows and give a better lesion segment.  But due complexity of code, it doesn't perform well.

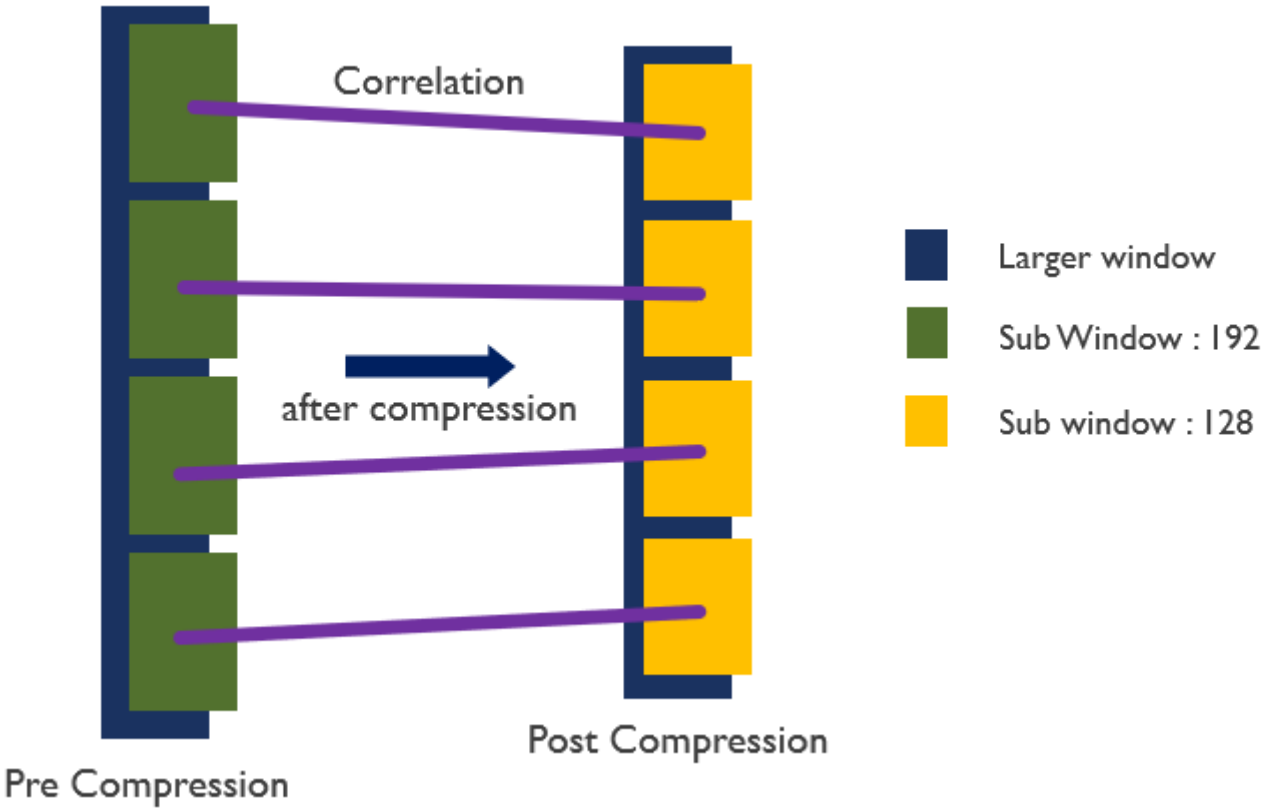


*Figure 4:12 Short term correlation with variable windows*

## 4.6 Steps for Modified Short term correlation:

1. Now the Smaller pre-compression sub window was taken 192 and the post-compression sub window were taken 128.

2. Then the corresponding sub windows from pre and post compression windows are correlated.

Rest Steps 3 – 12 as like before.

The short-term correlation algorithm was experimentally tested using:

- Mean (Constant overlap = 10px, Variable windows = 48px, 64px, 80px)
- Median (Constant overlap = 10px, Variable windows = 48px, 64px, 80px)

Results of Short-term correlation

*Figure 4:13 Mean results*

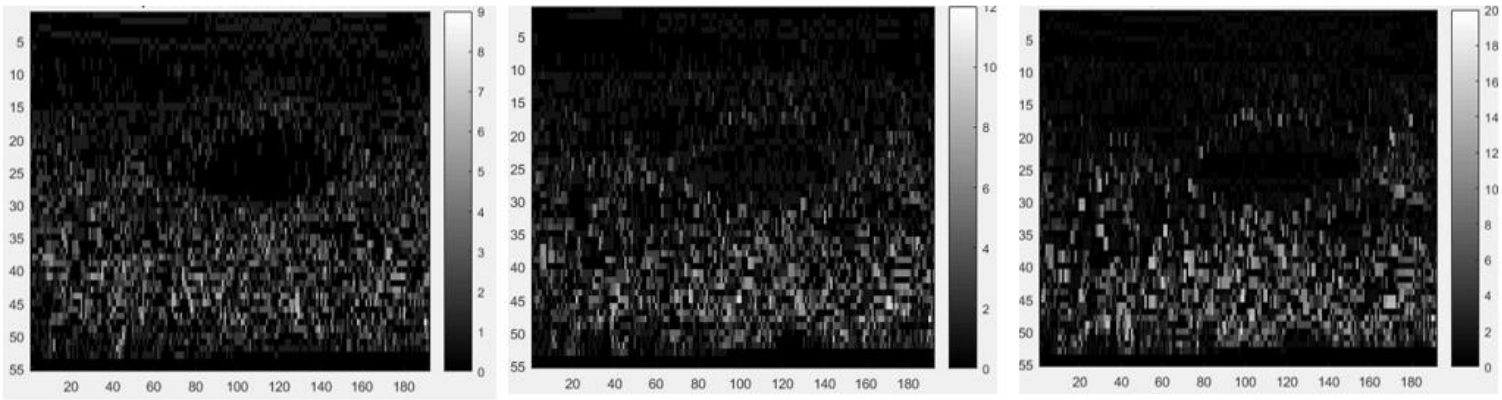

- Overlap 10
- Window 48

- Overlap 10
- Window 64

- Overlap 10
- Window 80

*Figure 4:14 Median results*

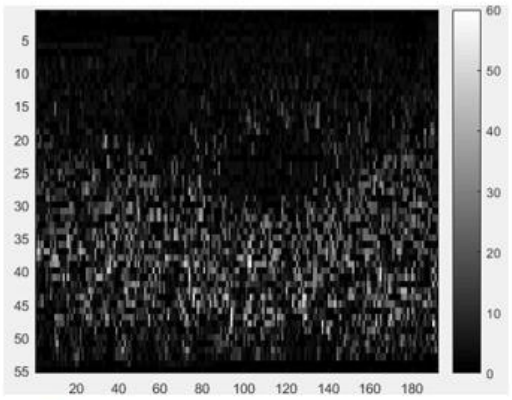

- Overlap 10
- Window 48

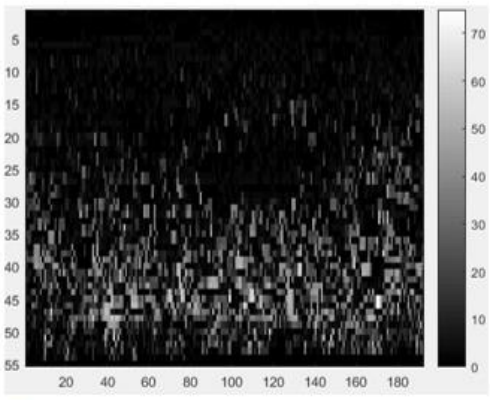

- Overlap 10
- Window 64

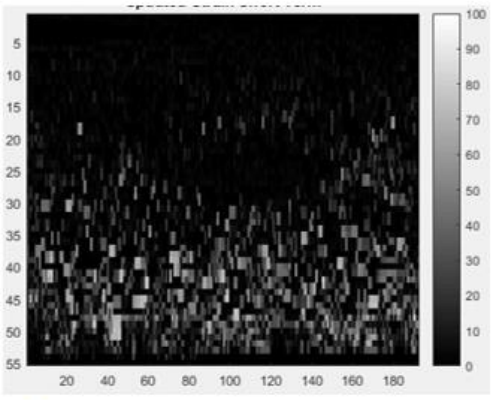

- Overlap 10
- Window 80

Conclusion to short term correlation:

1. Taking mean of the correlation among the sub windows gives better result than taking median.
2. In both the case of mean and median, taking smaller sub windows produces better results.
3. Using variable window sizes, we get better results in identifying the lesion.

# 5 Adaptive stretching along with 2D strain estimation method

## 5.1 Adaptive Stretching

In elastography, in addition to the electronic noise, a principal source of estimation error is the decorrelation of the echo signal as a result of tissue compression [46]. Temporal stretching of post compression signals previously was shown to reduce the decorrelation noise. In this technique, a novel estimator is introduced that uses the stretch factor itself as an estimator of the strain. It uses an iterative algorithm that adaptively maximizes the correlation between the pre- and post-compression echo signals by appropriately stretching the latter.

Conventional elastography [47] is a gradient based method, where the strain is estimated from the first difference of the time delays between two successive signal segments.

The gradient operation introduces significant amount of noise into the strain estimates, especially for small correlation window sizes and/or large overlap between the successive correlation windows.

However, to increase resolution, using a small correlation window size is desirable; moreover, to track rapid changes in elasticity, large window overlap may be used. In this article, we propose a novel estimator based on temporal stretching [48], [49] of the post compression echo signals.

## 5.2 2D Strain estimation

Clinical US scanners typically provide only 2-D images, only a few 2-D techniques have been reported to date. Most of them model 2-D local displacement as a translation in both axial and lateral (perpendicular to the US beam's propagation axis in the image plane) directions, and then compute strain estimates as the displacement gradient. The simplest approach is the 2-D speckle tracking [50].

After the physician applies a certain pressure with the transducer while sending the Ultrasound signal the muscles are displaced both in lateral and axial direction. By applying the 2D search method we try to find out how much the post compression data are shifted from the pre-compression data as a consequence of the muscle or tissue displacement.

On a different note, we can consider 2D Strain estimation method as a technique which combines both 1D and 1.5D in its operation.

## 5.3 METHOD OF APPLICATION:

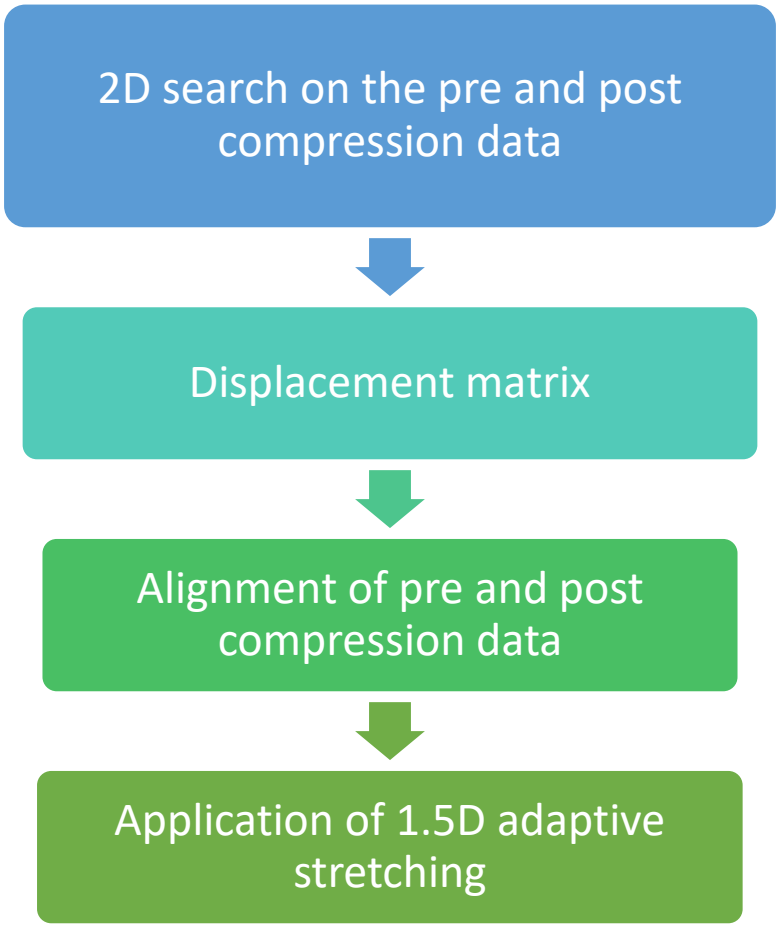

## 5.4 Explanation of operation:

In 2D search, both the lateral and axial shift of the post compression signal is taken into consideration together. Here, two-dimensional window of pre and post compression data are taken and correlation is performed throughout the pre-compression window until the maximum correlation is found.

The post compression window is taken such that it is larger in size laterally and smaller in size axially compared to the pre-compression window. It is chosen in this specific manner because after the application of strain body muscle and tissues deform in similar pattern.

This gives the information about how much the post compression data shifted from the pre-compression one. From this the post and pre-compression data can be aligned using the displacement matrix. 1.5D adaptive stretching is applied on the new aligned data and then strain estimation is performed.

This leads to the strain estimation of a post compression data with its corresponding pre-compression data, which if not aligned using 2D displacement matrix would not be possible.

Axial displacement

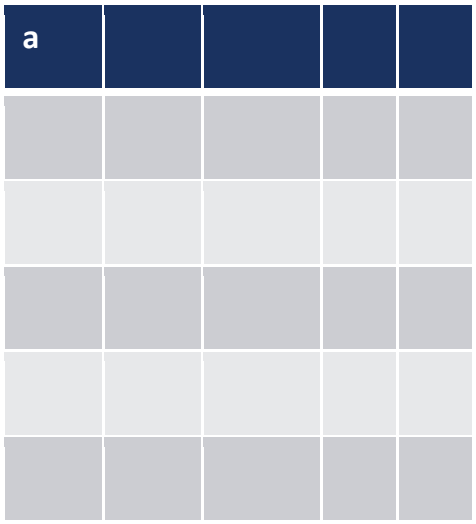


Pre-compression data

Lateral displacement

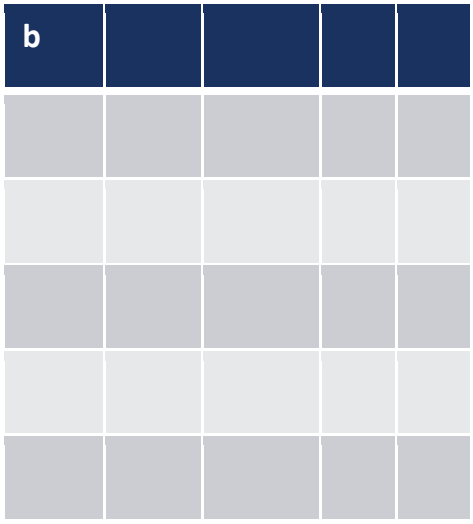


Post-compression data

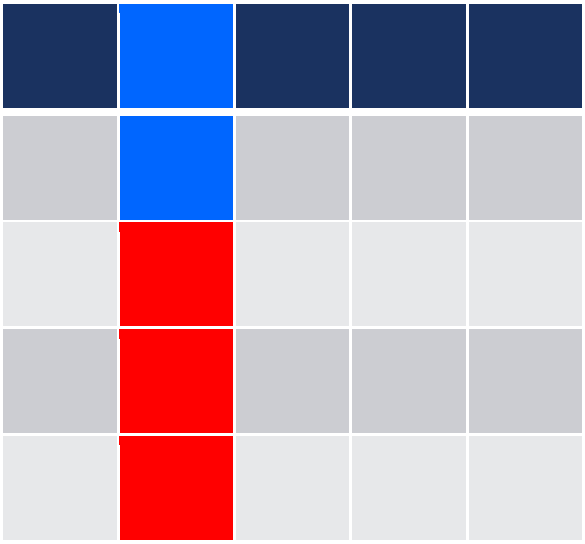

Shifted window (“a” units axially, “b” units laterally)

For the first window of the pre-compression data, the post compression data is shifted “a” rows axially and “b” columns laterally so that now 1.5D adaptive stretching takes place between aligned pre and post data.

## 5.5 RESULTS:

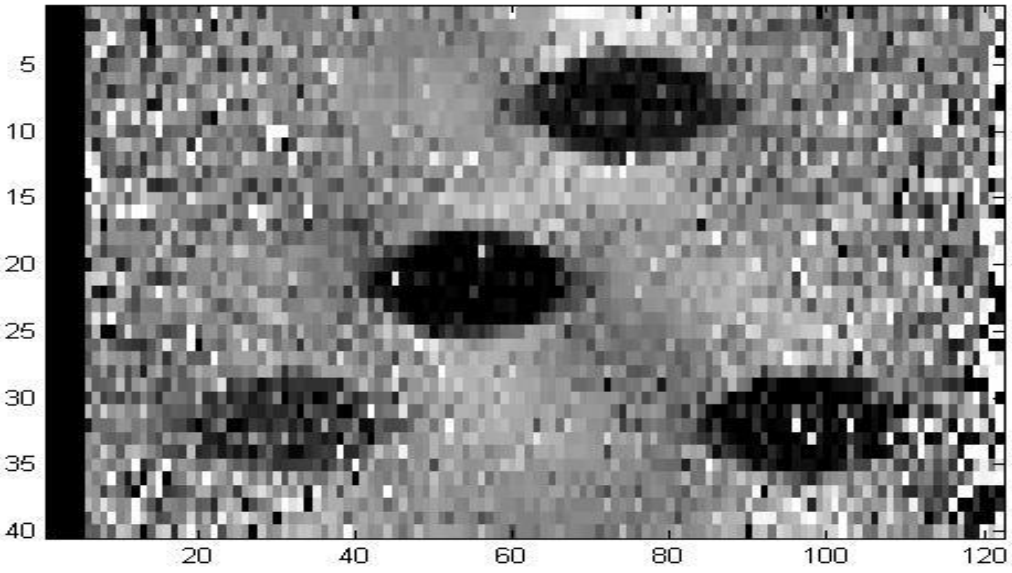


(a)

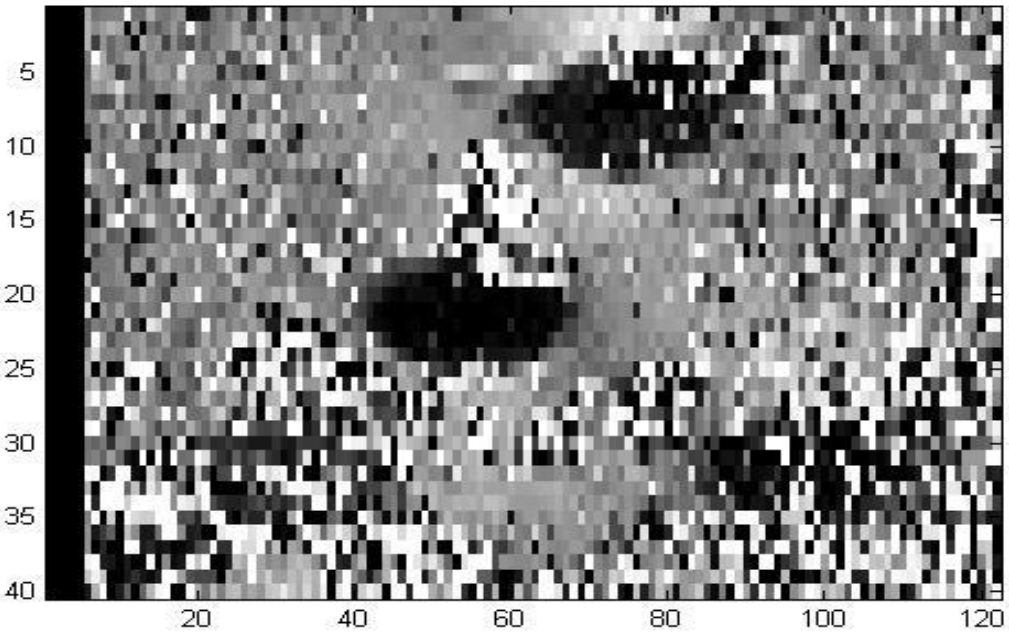


(b)

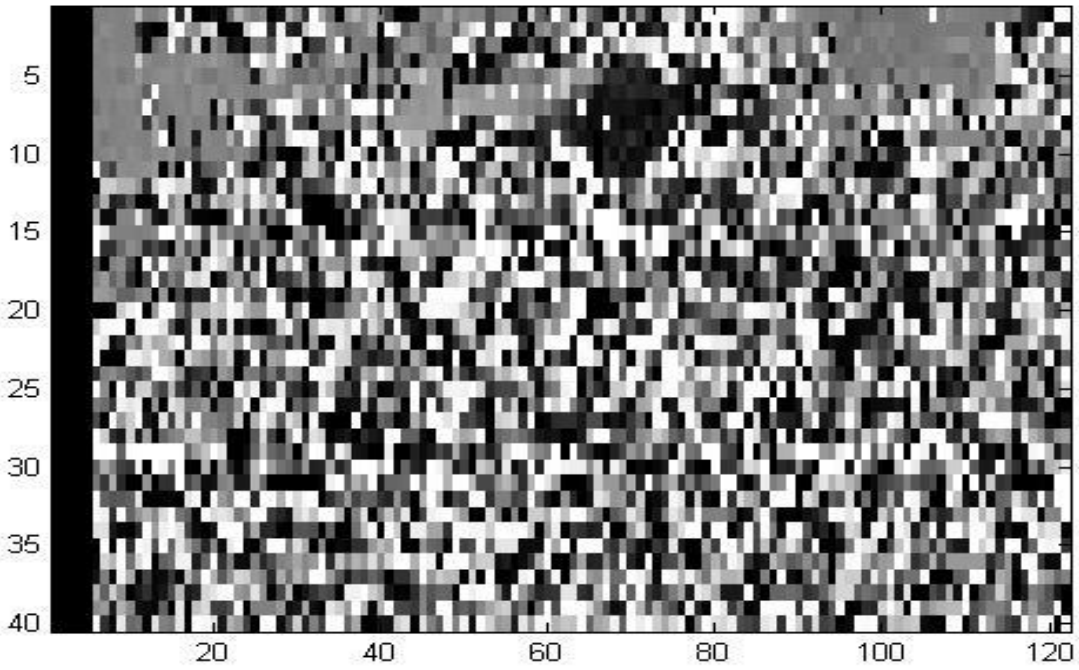


( c )

*Figure 5:1 processed data at different applied: (a) at 1% strain (b) at 2% strain (c) at 4% strain*

The result suggests that as percentage of applied strain increases the number of clearly visible lesions decreases. Usually the strain applied by physicians are not more than 2% so the results above 2% are not of major concern here.

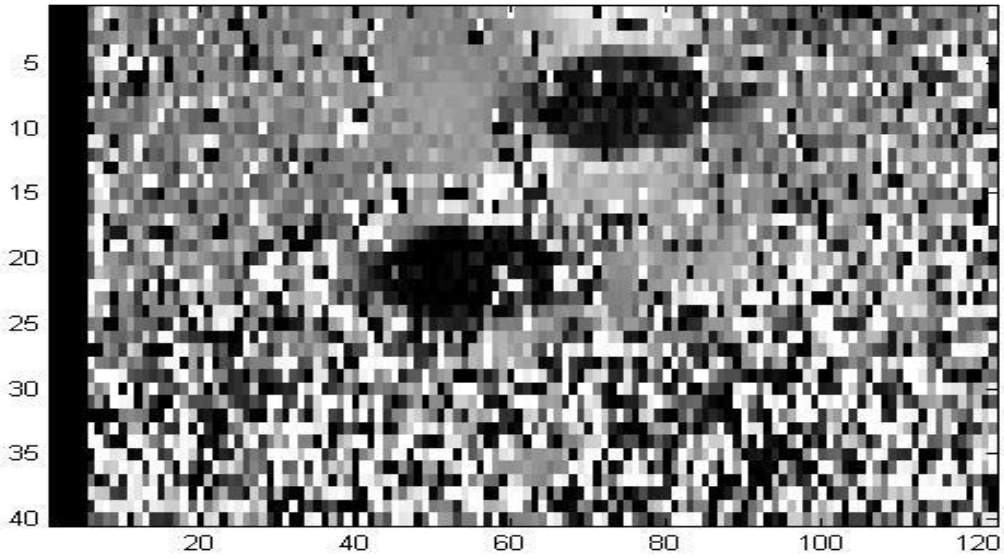
5
10
15
20
25
30
35
40
20
40
60
80
100
120

(a)

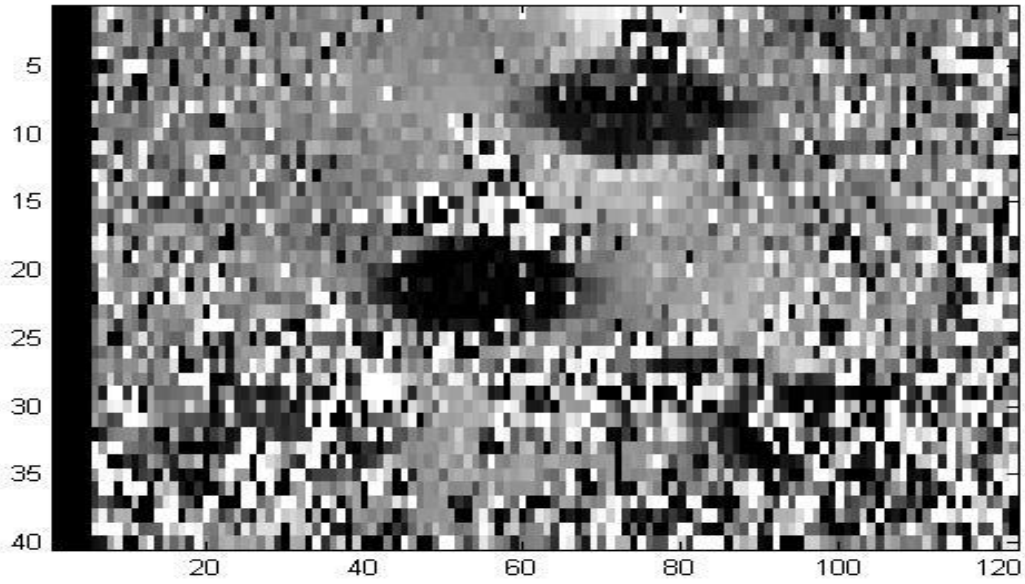
5
10
15
20
25
30
35
40
20
40
60
80
100
120

(b)

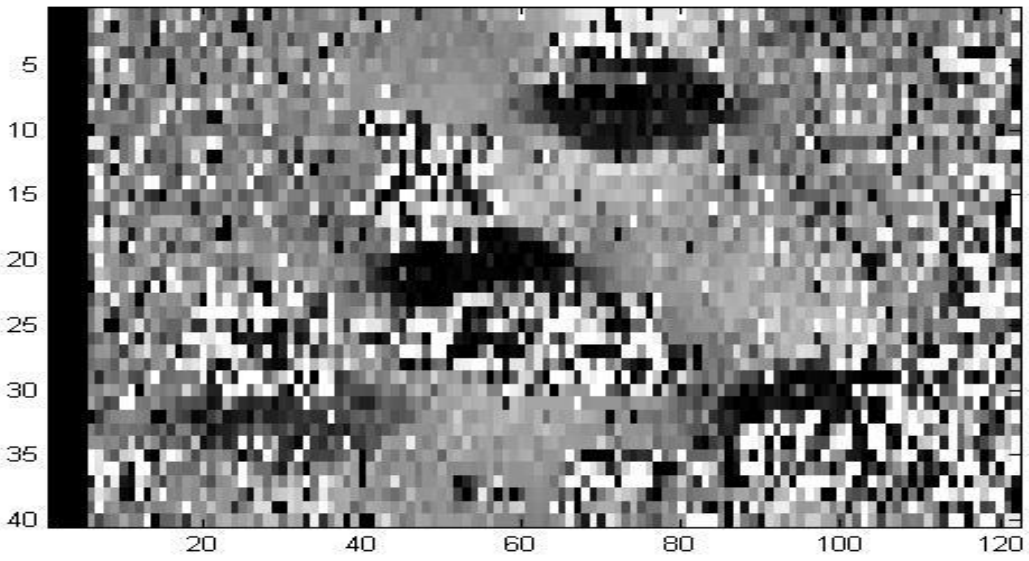


(c)

*Figure 5:2 Processed data at different post window size at 2% strain: (a) row size-8, column size-12 (b) row size-16, column size-24 (c) row size-32, column size-40*

The results above show the effect of post window size on the detection of lesion. It is observed that as post window size increased the visibility of lesions increased.

# 6 Breast Lesion Segmentation

## 6.1 Ultrasound Image Segmentation:

ULTRASOUND (US) image segmentation is strongly influenced by the quality of data. There are characteristic artefacts which make the segmentation task complicated such as attenuation, speckle, shadows, and signal dropout; due to the orientation dependence of acquisition that can result in missing boundaries. Automatically detecting tumors and extracting lesion boundaries in ultrasound images is difficult due to their specular nature and the variance in shape and appearance of sonographic lesions. Past work on automated ultrasonic breast lesion segmentation has not addressed important issues such as shadowing artifacts or dealing with similar tumor like structures in the sonogram. Further complications arise as the contrast between areas of interest is often low. However, there have been recent advances in transducer design, spatial/temporal resolution, digital systems, portability, etc., that mean that the quality of information from an ultrasound device has significantly improved [51],[60],[61]. This has led to increased use of ultrasound in not only its traditional area of application, diagnosis (and CAD), but also emerging areas such as image-guided interventions and therapy. Thus, there is currently a re-emergence of interest in understanding how to do one of the oldest image processing tasks, image segmentation, applied to ultrasound data.

In our study, we focused on detecting masses which could either be benign cysts or malignant tumors. Toward this end, we concentrated on three different sonographic features in order to help us distinguish the masses from glandular and fatty tissue and posterior acoustic shadowing.[62],[63] We used the spatial distribution of the various anatomic structures within the breast, echogenicity of the lesion, and its internal echo

pattern, as our three discriminating sonographic features. With the ultrasound transducer placed on the ROI, the lesion appears roughly in the middle of the image. The skin appears as a bright linear echo near the top of the image. Subcutaneous fat typically appears just below the skin region. Coopers ligaments appear as septum-like or tent-like structures that arise from the surface of the breast parenchyma. The glandular region is separated from the subcutaneous fat by the superficial fascia. The ribs appear in the lower most part of the image and are associated with dense posterior acoustic shadowing [52]. Internal echo pattern refers to the texture or arrangement of echoes within a focal sonographic lesion. A nonhomogeneous arrangement with few echoes, or even more, is suspicious for malignancy. A homogeneous internal echo pattern is more characteristic of subcutaneous fat. The echogenicity of a focal lesion is assessed in relation to the echo characteristics of adjacent tissues. The various grades of echogenicity are stated in reference to known structures, i.e., fat and glandular tissue. If a focal lesion appears less echogenic than fat, it is described as “almost anechoic.” Such a lesion would appear darker than the surrounding fatty tissue. A “hypoechoic” focal lesion is less echogenic than glandular structures but more echogenic than fat (i.e., it appears darker than the glandular tissue but lighter than the fatty tissue). “Isoechoic” closely approximates the echogenicity of the glandular structures, while “hyperechoic” is used when the focal lesions appear brighter than the surrounding glandula tissue. Hence, both cysts and malignant lesion appear darker than glandular tissue or fat which are usually either isoechoic or hyperechoic. Subcutaneous fat, on the other hand, is usually hypoechoic.

## 6.2 Work Flowchart:

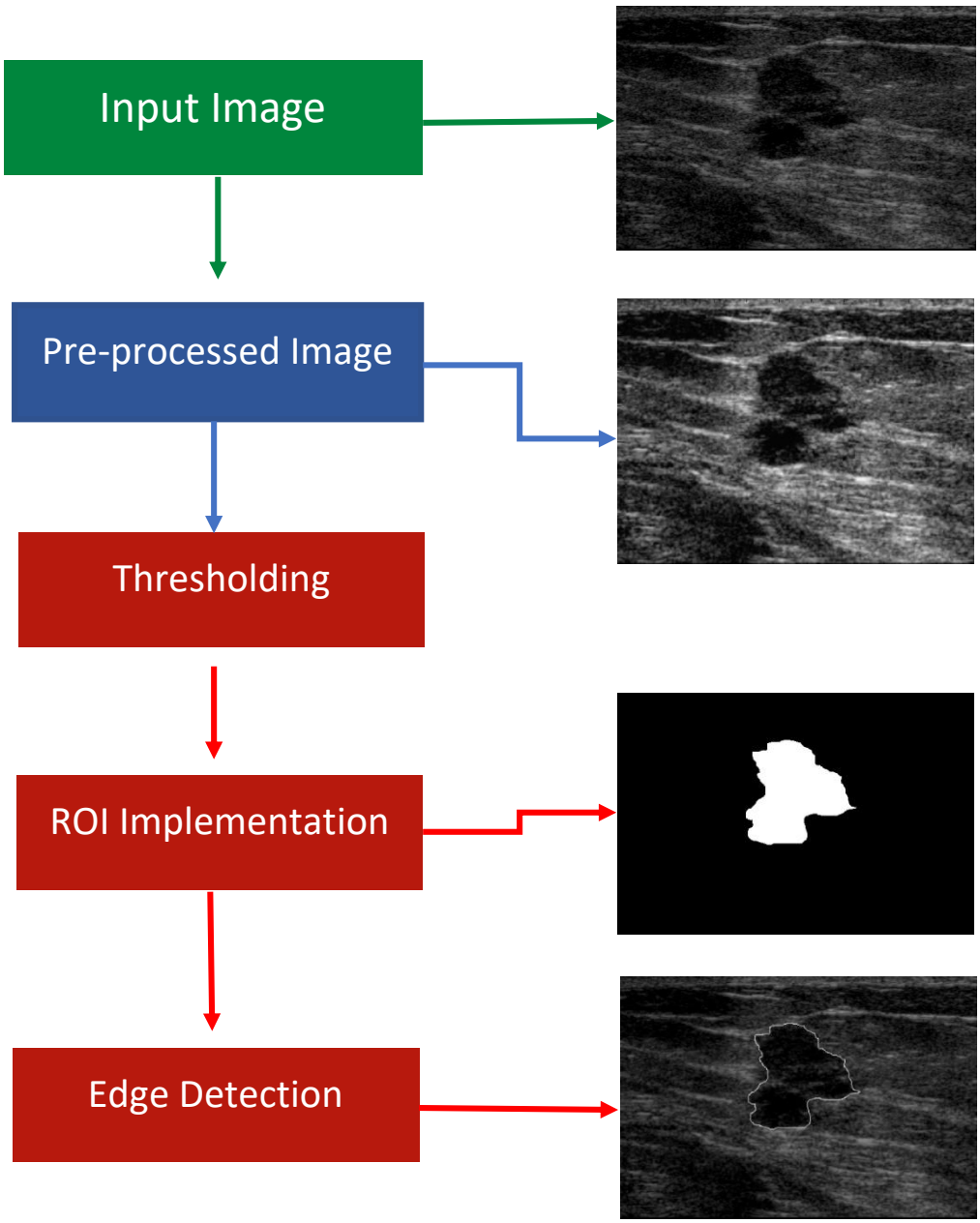


-

There are several steps of image segmentation technique.

- Gray level thresholding
- Automatic ROI generation
- Edge detection

## 6.3 Gray level thresholding:

We used a basic thresholding technique to create the segmented binary image. The pixels having gray level intensity greater than threshold value are in the foreground region. The pixels having gray level intensity less than threshold value are in the background region.

To select the thresholding value, we iteratively select thresholds based on the histogram and breast lesion's spatial characteristics. No training or empirical based threshold value is needed. The advantage of this iterative method is that it can be used for a US image without any requirement for image resource consistence or human interaction to tune a reasonable threshold value. Only the information of current US image is needed to determine the proper threshold.

We first calculate all the local minimums of the image histogram. A good threshold which can properly separate the lesion from the background should be one of these local minimums. Starting from the smallest to biggest, we evaluate every local minimum until we find the proper one. The iteration is described below: 1. Let t equal to the current local minimum of the histogram. Binarize and reverse the de-speckled image using threshold t (lesion becomes white and background is black) to get Ib. If the ratio of the number of foreground points and the number of background point is less than 0.1, let t equal to next local minimum. Continue until the ratio is no less than 0.1. 2. Perform

dilation and erosion on Ib to remove noise. 3. Find all the connected components in Ib. If none of the connected components has intersection with the image center region (a window about 1/2 size of the whole image and centered at the image center), let t equal to the next local minimum. Continue until there is a connected component has intersection with the center window. After applying the above 3 steps, a proper threshold t is chosen to binarize the image into background and foreground. Because the iterative threshold chosen process starts from the smallest local minimum and increases gradually based on the possible lesion to image ratio, it can avoid the problems that foreground is too large (lesion is connected with other tissues) or too small (lesion is not included into the foreground).

## 6.4 Automatic ROI generation

Since BUS images contain many different structures (tissues, fat, muscles, etc.) and the lesion area is usually a small part of the entire image, finding the region-of interest (ROI) is quite helpful for improving the speed and accuracy of segmentation. There are two typical ROI definitions: some papers defined ROI as an initial contour of the lesion (Liu et al. 2009; Madabhushi and Metaxas 2003)[53],[54], while others defined ROI as a rectangle region containing both lesion and some background information (Joo et al. 2004; Yap et al. 2008).[55],[56] In this article, we use the second definition and develop an automatic ROI generation method consisting of two parts: automatic seed point selection and region growing. Region growing is chosen because of its simplicity and fast speed. The accuracy of region growing method is not high enough for BUS images. However, the aim of ROI generation is only roughly locating the lesion rather than finding the accurate boundary. Therefore, region growing fits the purpose very well.

## 6.5 Edge Detection:

Delete the boundary – connected regions. After binarization, we find all the connected components. Each connected component represents a possible lesion region. Besides the real lesion, there are some regions connected with the boundary and they always have big areas. If a boundary region does not intersect with the center window (a window about 1/2 size of the entire image and located at the image center), this region is deleted from the lesion candidate list.

Now the left regions are either not connected with the boundary or having intersection with the image center window. We use the following score formula to

Rank each left regions. The one with the highest score is considered as the lesion region.

$$S_n = \frac{\sqrt{area}}{dis(C_n, C_0) * var(C_n)}; \qquad n = 1, \ldots, k$$

Where k is the number of regions, Area is the number of pixels in the region, Cn is the center of the region, C0 is the center of the image, and var(Cn) is the variance of a small circular region centered at Cn. In the implementation, we slightly moved the image center C0 to the upper part of the image (around row/4) based on our observation that a lesion frequently appears in the upper part of an image and shadow frequently appears in the lower part of an image. [57],[58]

## 6.6 Results:

In the first case we can see the boundary Is well detected. The boundary is complex in size. From this we can say that it is malignant or cancerous.[59] This decision can with more surety by doing quantitative analysis.

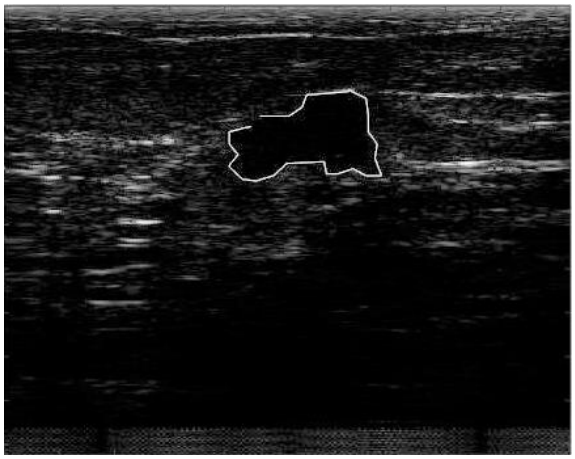

*Figure 6:1 Case 1*

For the second case the boundary is also well detected. The region is uniform and regular in size. We can predict that it is benign or non-cancerous lesion.

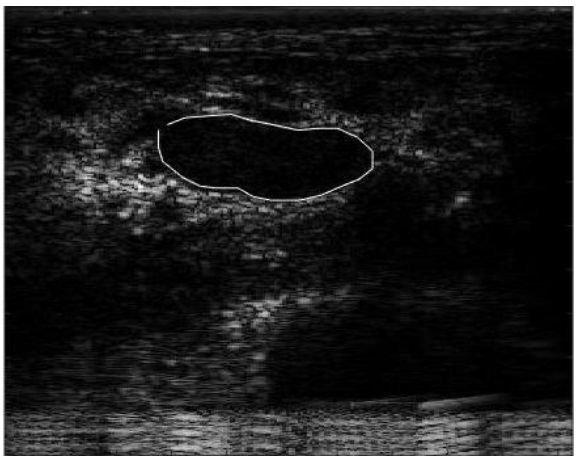

*Figure 6:2 Case 2*

The third case is similar to the second case. It's boundary is also well & regular in size which hints that it is probably non-cancerous.

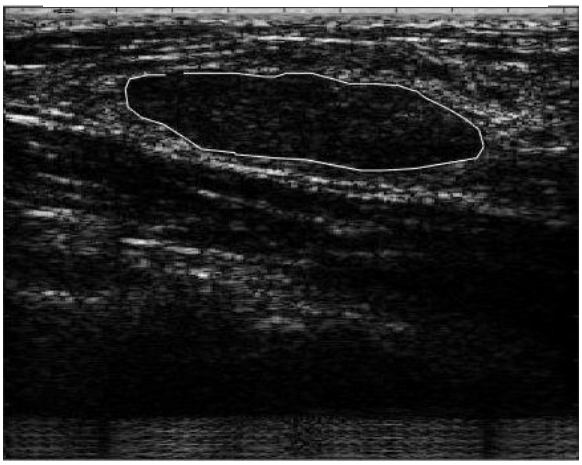

*Figure 6:3 Case 3*

In the fourth case, it could detect only one lesion region where we can see that there are two lesions. Decisions about the lesion can't be taken from this segmented image.

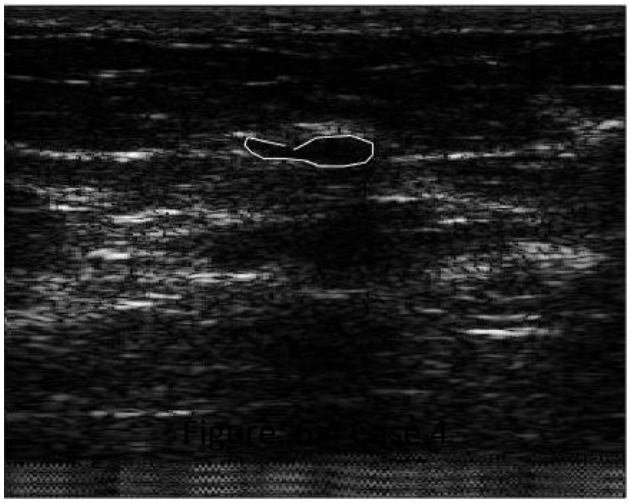

*Figure 6:4 Case 4*

The algorithm detected the boundary coordinates completely wrong this time. The reason behind this is probably there is no well defined lesion in this image.

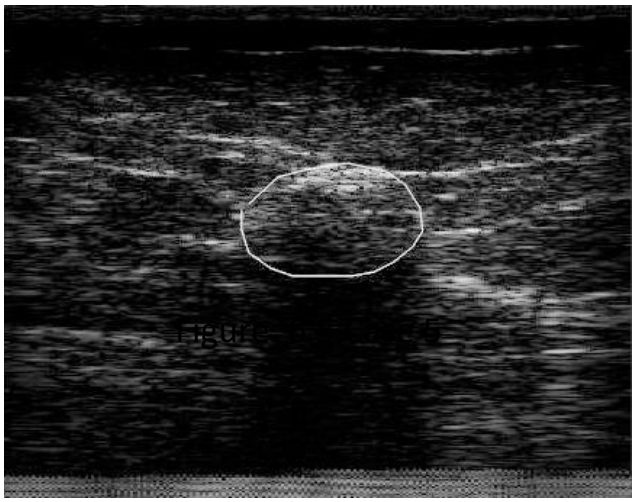

*Figure 6:5 Case 5*

In case six, the lesion area also consists some white parts inside the boundary which is completely wrong. So there is scope for further improvement in this algorithm.

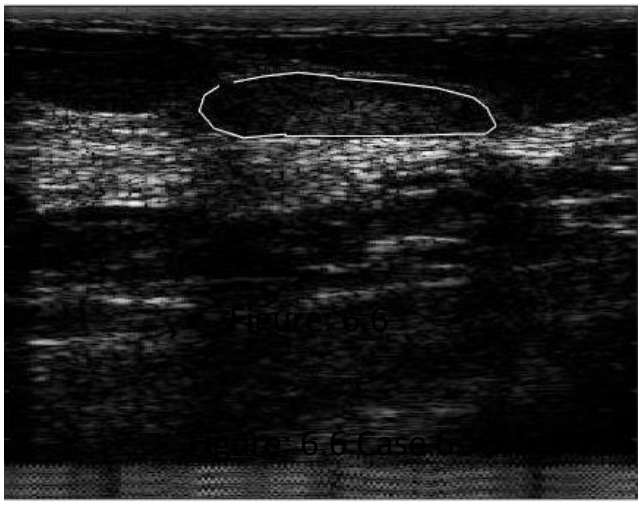

*Figure 6:6 Case 6*

# 7 Conclusion and Future scope of research:

Diagnosis of breast cancer has been widely improved since the development of high-resolution ultrasound equipment. In the past, ultrasound was only considered useful for the diagnosis of cysts. Meanwhile, it improves the differential diagnosis of benign and malignant lesions, local preoperative staging and guided interventional diagnosis.

We proposed a method to improve breast cancer detection by using various strain estimation methods and Image segmentation on ultrasound Images which would produce a well processed breast lesion. From the shape and orientation of the lesion physician can comment on the nature of the tumor. Which would lead to further treatment that could be started accordingly.

There are significant improvements possible in our method. So some of our future work will include the followings:

- The proposed wavelet filter can decompose only up to 2 level, in future we will try to increase the level of decomposition for fine scale analysis.
- The proposed 2D search method works well only for strain less than 2%, in future we will try to make it work well with increased applied strain.
- The adaptive stretching method used was in time domain, in future we would like to apply it in frequency domain.
- The proposed segmentation technique does not identify imprecise and multiple lesions in a BUS image, we would like to develop our algorithm in such a way that lesions other than the significant ones could be identified as well in near future.

# 8 REFERENCES:


[1] https://www.wcrf.org/dietandcancer/cancer-trends/breast-cancer-statistics

[2] http://www.who.int/cancer/detection/breastcancer/en/index1.html

[3] https://www.cancer.org/cancer/breast-cancer-in-men/about/key-statistics.html

[4] M. P. Coleman, M. Quaresma, F. Berrino, J.-M. Lutz, R. De Angelis, R. Capocaccia, et al., "Cancer survival in five continents: a worldwide population-based study (CONCORD)," The lancet oncology, vol. 9, pp. 730-756, 2008.

[5] Howlader N, Noone AM, Krapcho M, et al. SEER Cancer Statistics Review, 1975-2014. https://seer.cancer.gov/csr/1975_2014/, based on November 2016 SEER data submission, posted to the SEER web site, April 2017. Bethesda, MD: National Cancer Institute, 2017.

[6] Surveillance, Epidemiology, and End Results (SEER) Program (www.seer.cancer.gov) SEER*Stat Database: Incidence – SEER 18 Regs Research Data, Nov 2016 Sub (2000-2014) <Katrina/Rita Population Adjustment> – Linked To County Attributes – Total U.S., 1969-2015 Counties, National Cancer Institute, DCCPS, Surveillance Research Program, released April 2017, based on the November 2016 submission

[7] B. Sahiner, H.-P. Chan, M. A. Roubidoux, L. M. Hadjiiski, M. A. Helvie, C. Paramagul, et al., "Malignant and Benign Breast Masses on 3D US Volumetric Images: Effect of Computer-aided Diagnosis on Radiologist Accuracy 1," Radiology, vol. 242, pp. 716-724, 2007.

[8] K. Drukker, M. L. Giger, K. Horsch, M. A. Kupinski, C. J. Vyborny, and E. B. Mendelson, "Computerized lesion detection on breast ultrasound," Medical physics, vol. 29, pp. 14381446, 2002.

[9] https://www.breastcancer.org/symptoms/testing/types/mri/how_performed

[10] Haas JS, Hill DA, Wellman RD, et al. Disparities in the use of screening magnetic resonance imaging of the breast in community practice by race, ethnicity, and socioeconomic status. Cancer. 2016;122: 611-617.

[11] Huay-BenPan'The Role of Breast Ultrasound in Early Cancer Detection',Journal of Medical Ultrasound, Volume 24, Issue 4, December 2016, Pages 138-141

[12] Y. Cheung, Y. Wan, S. Chen, et al, Sonographic evaluation of mammographic detected microcalcification without a mass prior to stereotactic core needle biopsy J Clin Ultrasound, 30 (2003), pp. 323-331

[13] T. A. Krouskop, D. R. Dougherty, and F. S. Vinson, “A pulsed Doppler ultrasonic system for making noninvasive measurements of the mechanical properties of soft tissue,” J. Rehabil. Res.Dev., vol. 24, pp. 1–8, 1987.

[14] R. M. Lerner and K. J. Parker, “Sono-elasticity in ultrasonic tissue characterization and echographic imaging,” inProc. 7th Eur. Comm. Workshop, J. M. Thijssen, Ed. Nijmegen, The Netherlands, 1987.

[15] R. M. Lerner, S. R. Huang, and K. J. Parker, “‘Sonoelasticity’images derived from ultrasound signals in mechanically vibrated tissues,” Ultrason. Med. Biol., vol. 16, pp. 231–239, 1990.

[16] Y. Yamakoshi, J. Sato, and T. Sato, “Ultrasonic imaging of internal vibration of soft tissue under forced vibration,” IEEE Trans. Ultrason., Ferroelect., Freq. Contr., vol. UFFC-47, pp. 45–53, 1990.

[17] J. Ophir, I. C´ espedes, H. Ponnekanti, Y. Yazdi, and X. Li, “Elastography: A method for imaging the elasticity in biological tissues,” Ultrason. Imaging, vol. 13, pp. 111–134, 1991.

[18] M. O’Donnell, A. R. Skovoroda, B. M. Shapo, and S. Y. Emelianov, “Internal displacement and strain imaging using ultrasonic speckle tracking,” IEEE Trans. Ultrason., Ferroelect., Freq. Contr., vol. UFFC-41, pp. 314–325, 1994.

[19] N. Duta and M. Sonka, “Segmentation and interpretation of MR brain images:Animprovedactiveshapemodel,” IEEETrans.Med.Imag.,vol. 17, pp. 1049–1062, Dec. 1998

[20] J. K. Udupa and S. Samarsekera, “Fuzzy connectedness and object definition: Theory, algorithms, and applications in image segmentation,” Graphical Models Image Processing, vol. 58, pp. 246–261, 1996.

[21] N. R. Mudigonda, R. M. Ragayyan, and J. E. Leo Desautels, “Gradient and texture analysis for the classification of mammographic masses,” IEEE Trans. Med. Imag., vol. 19, pp. 1032–1043, Oct. 2000.

[22] M. L. Giger et al., “Computerized analysis of lesions in ultrasound images of the breast,” Acad. Radiol., vol. 6, pp. 665–674, 1999.

[23] S.Sudha, G.R.Suresh and R.Sukanesh, “Speckle Noise Reduction in Ultrasound Images by Wavelet Thresholding based on Weighted Variance,” International Journal of Computer Theory and Engineering, Vol. 1, No. 1, April 2009 1793-8201

[24] D. Hillery, “Iterative wiener filters for Images restoration”. IEEE Transaction on SP, 39, pp. 1892-1899, 1991.

[25] MICHAEL UNSER, SENIOR MEMBER, IEEE, AND AKRAM ALDROUBI, “A Review of Wavelets in Biomedical Applications ,“ PROCEEDINGS OF THE IEEE, VOL. 84, NO.4, APRIL 1996

[26] Ten Lectures on Wavelets. Philadelphia, PA: Soc. Ind. and AppL Math., 1992

[27] M. Vetterli and J. Kovacevic, Wavelets and Subband Coding. Englewood Cliffs, NJ: Prentice Hall, 1995.

[28] D. L. Donoho and I. M. Johnstone, ” Ideal spatial adaptation via wavelet shrinkage” Biometrika, vol. 81, pp. 425–455, 1994.

[29] Denver, Fodor I. K, Kamath. C, ” Denoising Through Wavelet Shrinkage,” An Empirical Study, Journal of Electronic Imaging. 12, pp.151-160, 2003.

[30] D. L. Donoho and I. M. Johnstone, ”Adapting to unknown smoothness via wavelet shrinkage” Journal American Statistical. Association. vol. 90, no. 432, pp. 1200–1224, 1995

[31] https://www.sciencedirect.com/science/article/pii/S2211568413000302

[32] Catheline S. “Interférométrie-speckle ultrasonore : application à la mesure d’élasticité.” Thèse de doctorat. Université Paris VII, 1998.

[33] S. Catheline, J. Thomas, F. Wu, M. Fink, “Diffraction field of a low frequency vibrator in soft tissues using transient elastography,” IEEE Trans Ultrason Ferroelectr Freq Control, 46 (4) (1999), pp. 1013-1019

[34] Gennisson JL. Le palpeur acoustique : “un nouvel outil d’investigations des tissus biologiques”. Thèse de l’université Pierre-et-Marie-Curie Paris-6, 2003.

[35] J.L. Gennisson, S. Catheline, S. Chaffaï, M. Fink, “Transient elastography in anisotropic medium: application to the measurement of slow and fast shear waves velocities in muscles," J Acoust Soc Am, 114 (1) (2003), pp. 536-541

[36] S. Catheline, J.L. Gennisson, G. Delon, R. Sinkus, M. Fink, S. Abouelkaram, *et al.* *“*Measurement of viscoelastic properties of homogeneous soft solid using transient elastography: an inverse problem approach,” J Acoust Soc Am, 116 (6) (2004), pp. 3734-3741

[37] S. Catheline, J.L. Gennisson, M. Fink, Measurement of elastic non-linearity of soft solid with transient elastography,” J Acoust Soc Am, 114 (6) (2003), pp. 3087-3091

[38] J Ophir, S K Alam, B Garra, F Kallel, E Konofagou, T Krouskop and T Varghese , “Elastography: ultrasonic estimation and imaging of the elastic properties of tissues“.

[39] Fung Y.C., “Biomechanical Properties of Living Tissues,” Springer-Verlag, New York, 1981, Chapter 7

[40] Anderson W.A.D., Pathology, C.V. Mosby, St. Louis, 1953.

[41] Jonathan OPHIR , Faouzi KALLEL, Tomy VARGHESE , Elisa KONOFAGOU, S. Kaisar ALAM , Thomas KROUSKOP, Brian GARRA , Raffaella RIGHETTI, “IMAGERIE ACOUSTIQUE ET OPTIQUE DES MILIEUX BIOLOGIQUES OPTICAL AND ACOUSTICAL IMAGING OF BIOLOGICAL MEDIA”.

[42] Mark A. Lubinski*,* Stanislav *Y .* Emelianov*,* and Matthew O’Donnell, *“*Speckle Tracking Methods for Ultrasonic Elasticity Imaging Using Short-Time Correlation,” IEEE TRANSACTIONS ON ULTRASONICS, FERROELECTRICS, AND FREQUENCY CONTROL, VOL. 46, NO. 1, JANUARY 1999

[43] J. W. Betz, “Comparison of the deskewed short-time correlatorand the maximum likelihood correlator,” *IEEE Trans. Acoust., Speech, Signal Processing,* vol. ASSP-32, pp. 285-294, Apr. 1984

[44] M. A. Lubinski, S.Y. Emelianov, A. R. Skovoroda, and M. O’Donnell, “Imaging lateral displacements using soft tissue incompressibility,” *Ultrason.* Imaging,, vol. 17, pp. 69-70, 1995.

[45] A. R. Skovoroda, M. A. Lubinski, S. *Y .* Emelianov, and hi. O’Donnell, “Nonlinear estimation of the lateral displacement using tissue incompressibility,” IEEE Trans. *Ult*

[46] S. Kaisar Alam, *Member, IEEE*, Jonathan Ophir, *Member, IEEE*, and Elisa E. Konofagou, “An Adaptive Strain Estimator for Elastography”, ieee transactions on ultrasonics, ferroelectrics, and frequency control, vol. 45, no. 2, march 1998

[47] J. Ophir, I. Cespedes, H. Ponnekanti, Y. Yazdi, and X. Li, “Elastography: A method for imaging the elasticity in biological tissues",Ultrason. Imaging, vol. 13, pp. 111-134, 1991.

[48] I. Cespedes, “Elastography: imaging of biological tissue elasticity,"Ph.D. dissertation, Univ. Houston, Houston, TX, 1993.

[49] S. K. Alam and J. Ophir, “Reduction of signal decorrelation from mechanical compression of tissues by temporal stretching|applications to elastography," Ultrason. Med. Biol., vol. 23, no. 1, pp. 95{105, 1997.

[50] Elisabeth Brusseau*, Jan Kybic, Jean-François Déprez, and Olivier Basset, “2-D Locally Regularized Tissue Strain Estimation from Radio-Frequency Ultrasound Images: Theoretical Developments and Results on Experimental Data “, IEEE TRANSACTIONS ON MEDICAL IMAGING, VOL. 27, NO. 2, FEBRUARY 2008

[51] S. L. Bridal, J.-M. Correas, A. Saied, and P. Laugier, “Milestones on the road to higher resolution, quantitative, and functional ultrasonic imaging,” Proc. IEEE, vol. 91, no. 10, pp. 1543–1561, Oct. 2003

[52] W. Leucht and D. Leucht, Teaching Atlas of Breast Ultrasound. New York: Thieme Medical, 2000, pp. 24–38

[53] Anant Madabhushi and Dimitris N. Metaxas," Combining Low-, High-Level and Empirical Domain Knowledge for Automated Segmentation of Ultrasonic Breast Lesions." IEEE TRANSACTIONS ON MEDICAL IMAGING, VOL. 22, NO. 2, FEBRUARY 2003

[54] Liu B, Cheng HD, Huang J, Tian JW, Liu J, Tang XL. "Automated segmentation of ultrasonic breast lesions using statistical texture classification and active contour based on probability distance." Ultrasound Med Biol 2009;35:1309–1324.

[55] Joo S, Yang YS, Moon WK, Kim HC. "Computer-aided diagnosisof solid breast nodules: Use of an artificial neural network based on multiple sonographic features." IEEE Trans Med Imaging 2004;23: 1292–1300.

[56] Yap MH, Edirisinghe EA, Bez HE. "A novel algorithm for initial lesion detection in ultrasound breast images." JAppl Clin Med Phys 2008;9: 2741.

[57] JUAN SHAN, H. D. CHENG, and YUXUAN WANG, "Completely Automated segmentation approach for breast ultrasound images using multiple domain features ." Ultrasound in Med. & Biol., Vol. 38, No. 2, pp. 262–275, 2012

[58] Juan Shan, H. D. Cheng, Yuxuan Wang," A novel automatic seed point selection algorithm for breast ultrasound images," Dept. of Computer Science, Utah State University, Logan, UT 84322

[59] A. T. Stavros et al., "Solid breast nodules: Use of sonography to distinguish between benign and malignant lesions," Radiol., vol. 196, pp. 123–134, 1995.

[60] I.Dydenko,D.Friboulet,J.M.Gorce,J.D'hooge,B.Bijnens,andI.E. Magnin,"Towardsultrasoundcardiacimagesegmentationbasedonthe radiofrequency signal," Med. Image Anal., vol. 7, no. 3, pp. 353–367, 2003.

[61] O. Husby and H. Rue, “Estimating blood vessel areas in ultrasound imagesusingadeformabletemplatemodel,”Statist.Model.,vol.4,no. 3, pp. 211–226, 2004.

[62] P. H. Arger, C. Sehgal, E. Conant, J. Zuckerman, S. E. Rowling, and J. A. Paton, “Inter-reader variability and predictive value of US descriptions of solid breast masses,” Acad. Radiol., pp. 335–342, 2001.

[63] W. Leucht and D. Leucht, “Teaching Atlas of Breast Ultrasound.” New York: Thieme Medical, 2000, pp. 24–38.